Electronic Supplementary Material (ESI) for Dalton Transactions.

Supporting Information

Knock-on Synthesis of Tritopic Calix[4]pyrrole Host for Enhanced Anion Interactions

Mandeep K. Chahal, Jan Labuta, Václav Březina, Paul A. Karr, Yoshitaka Matsushita, Whitney A. Webre, Daniel T. Payne, Katsuhiko Ariga, Francis D'Souza and Jonathan P. Hill

Contents

Singular value decomposition (SVD) and determination of number of absorbing species

During titration experiment only a few absorbing species are present in the measured spectrum (e. g. free host, complex 1:1, complex 1:2, etc.). Measured spectra (absorbance values) from a titration experiment could be arranged into a $N_{res} \times N_{exp}$ matrix **A**, where N_{exp} is number of titration steps and N_{res} is number of discrete points each spectrum consists of.

Assuming spectral shape of these absorbing species is constant during the whole experiment, matrix **A** can be viewed as linear combination of matrix of absorbing species' spectra. This linear combination is expressed as a matrix product:

$$\mathbf{A}_{\lambda n} = \sum_{i=1}^{N_{spec}} \mathbf{Z}_{\lambda i}\, \mathbf{F}_{in} \qquad \text{(S1)}$$

where $\lambda = 1, 2 \ldots N_{res}$ and $n = 1, 2, \ldots N_{exp}$.

Columns of **Z** contain spectral shapes of absorbing species and rows of **F** contain their fractions during experiment (each column of **F** sums to 1). N_{spec} stands for number of present absorbing species (for example: N_{spec} =3 if only free porphyrin, complex 1:1 and complex 1:2 are present). Correct number of N_{spec} can be deduced from *singular value* decomposition (SVD)[S1-S4] procedure applied to the matrix **A**:

$$\mathbf{A}_{\lambda n} = \sum_{\mu=1}^{N_{res}} \sum_{m=1}^{N_{exp}} \mathbf{U}_{\lambda\mu} \mathbf{W}_{\mu m}\, \mathbf{V}_{mn} \qquad \text{(S2)}$$

where again $\lambda = 1, 2 \ldots N_{res}$ and $n = 1, 2, \ldots N_{exp}$.

Columns of the square orthonormal $N_{res} \times N_{res}$ matrix **U** are called basis spectra. **W** is a rectangular diagonal $N_{res} \times N_{exp}$ matrix. These numbers are denoted as singular values and are sorted in descending order. Rows of the square orthonormal $N_{res} \times N_{res}$ matrix **V** are called amplitude vectors. A convenient compact form of SVD is **A** = **UK** (where **K** = **WV**), where rows of **K** are called *combination coefficients*.

In the presence of N_{spec} absorbing species in the titration experiment, first N_{spec} basis spectra carry the information about spectral shape of the absorbing species, first N_{spec} amplitude vectors (or combination coefficients) carry the information about their fraction in the sample. Remaining parts of the matrices **U** and **V** or **K** represent noise. Using approximate transformation matrix basis spectra can be transformed into the matrix of absorbing spectra **Z** and amplitude vectors/combination coeff. into the matrix of fractions **F**[S1,S3,S5]

The presence of N_{spec} absorbing species causes first N_{spec} singular values to be substantially higher than the rest (holds for sufficiently high signal/noise ratio, N_{spec} is often denoted as the factor dimension). Another indicator is a plot of residuals that describes average standard error of the SVD approximation of measured spectra for given factor dimension. Residuals are defined as follows.[S2]

$$\mathrm{residual}(i) = \sqrt{\sum_{j=i+1}^{N_{exp}} \mathbf{W}_{jj}^2 \Big/ N_{res}(N_{exp} - i)} \qquad \text{(S3)}$$

For $i = N_{spec}$ the value of the residual drops significantly since all relevant spectra of absorbing species are included in SVD approximation of **A**. For $i > N_{spec}$ the value of residual does not change much since only basis vectors which consists mostly of noise are added into SVD approximation. Signal containing basis and amplitude vectors also tend to have higher autocorrelation compared to noise containing vectors.

The simplest case N_{spec} = 2 can be easily identified observing plot of mutual dependence of the first two combination coefficients which should be linear.[S6]

Table S1. Overall results of binding properties of **1** and Bn_2OxP as obtained from analysis of UV-vis and NMR titration experiments with various anions. Intervals of acceptable values salt dissociation constants K_d and host-anion binding constants K_A.

Host	TBA anion	Acceptable range[a]		Best fit[b]	
		K_d / M	K_A / M^{-1}	K_d / M	K_A / M^{-1}
1	Cl^- [c]	$3.8\times10^{-6} - 7.0\times10^{-5}$	$1.5\times10^{5} - 6.0\times10^{5}$	1.6×10^{-5}	2.1×10^{5}
1	NO_3^-	$5.0\times10^{-5} - 1.4\times10^{-3}$	$1.4\times10^{5} - 2.0\times10^{5}$	1.4×10^{-4}	1.5×10^{5}
1	ClO_4^-	$2.5\times10^{-4} - 6.7\times10^{-4}$	$1.2\times10^{4} - 1.9\times10^{4}$	3.9×10^{-4}	1.5×10^{4}
1	HSO_4^-	$< 1.0\times10^{-6}$	$> 3.3\times10^{6}$	----	----
Bn_2OxP	Cl^- [c]	$1.6\times10^{-6} - 2.2\times10^{-5}$	$2.8\times10^{4} - 2.1\times10^{5}$	6.9×10^{-6}	6.7×10^{4}
Bn_2OxP	NO_3^-	$7.0\times10^{-5} - 2.0\times10^{-4}$	$1.7\times10^{4} - 2.7\times10^{4}$	1.2×10^{-4}	2.2×10^{4}

[a] Acceptable range of K_d and K_A values as determined by simultaneous analysis of NMR and UV-vis data.
[b] Best fit denotes the value of of K_d and K_A at which the total sum of squares (TSS) was minimal.
[c] Dissociation constant for TBACl is $K_d = 1.6 (\pm 0.2) \times 10^{-5}$ M in CH_2Cl_2 (at 22 °C).[S7]

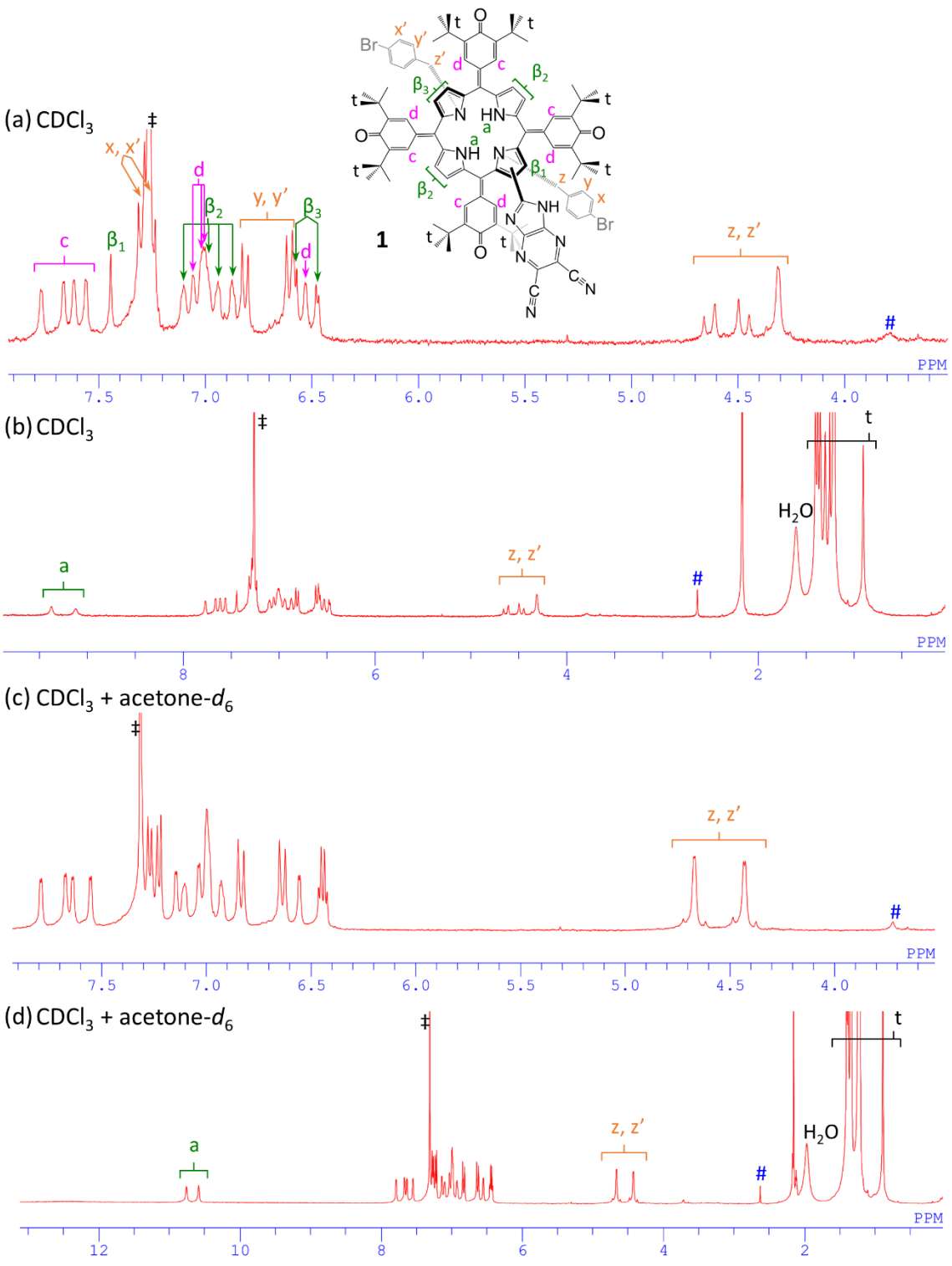

Figure S1. ^{1}H NMR spectra assignment of **1** (2 mM, 25 °C). (a) Aromatic portion of spectrum in neat $CDCl_3$ solvent. (b) Whole spectrum in neat $CDCl_3$ solvent. (c) Aromatic portion of spectrum in $CDCl_3$ with addition of acetone-d_6. (d) Whole spectrum in $CDCl_3$ with addition of acetone-d_6. Hash mark (#) denotes impurities. Double dagger mark (‡) denotes residual $CHCl_3$.

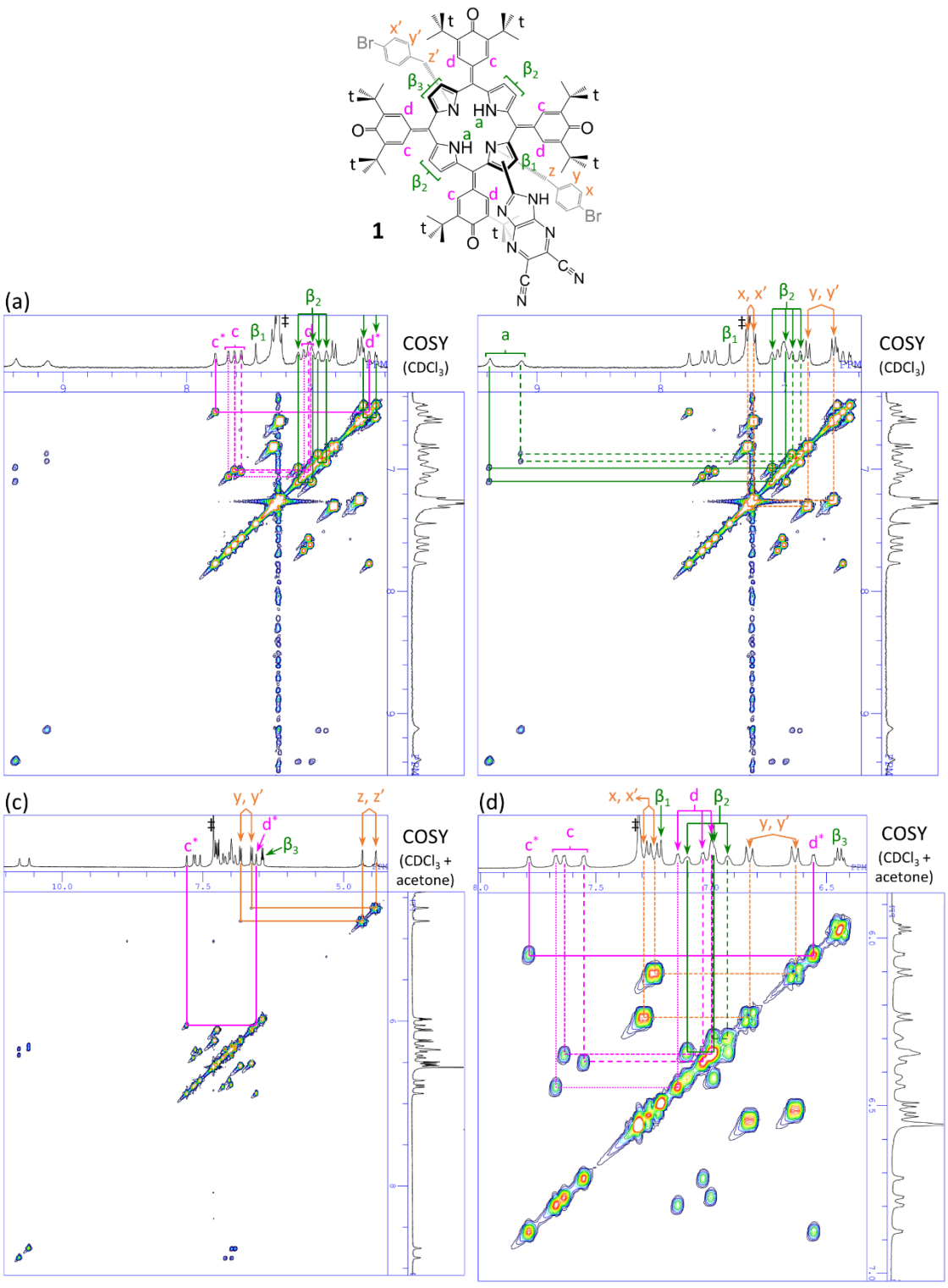

Figure S2. ^{1}H-^{1}H COSY NMR spectra of **1** (2 mM, 25 °C) in (a,b) $CDCl_3$ and in (c,d) $CDCl_3$ with addition of acetone-d_6. c*and d* resonances are both at one of the hemiquinonoid groups adjacent to imidazole group. Double dagger (‡) mark denotes residual $CHCl_3$.

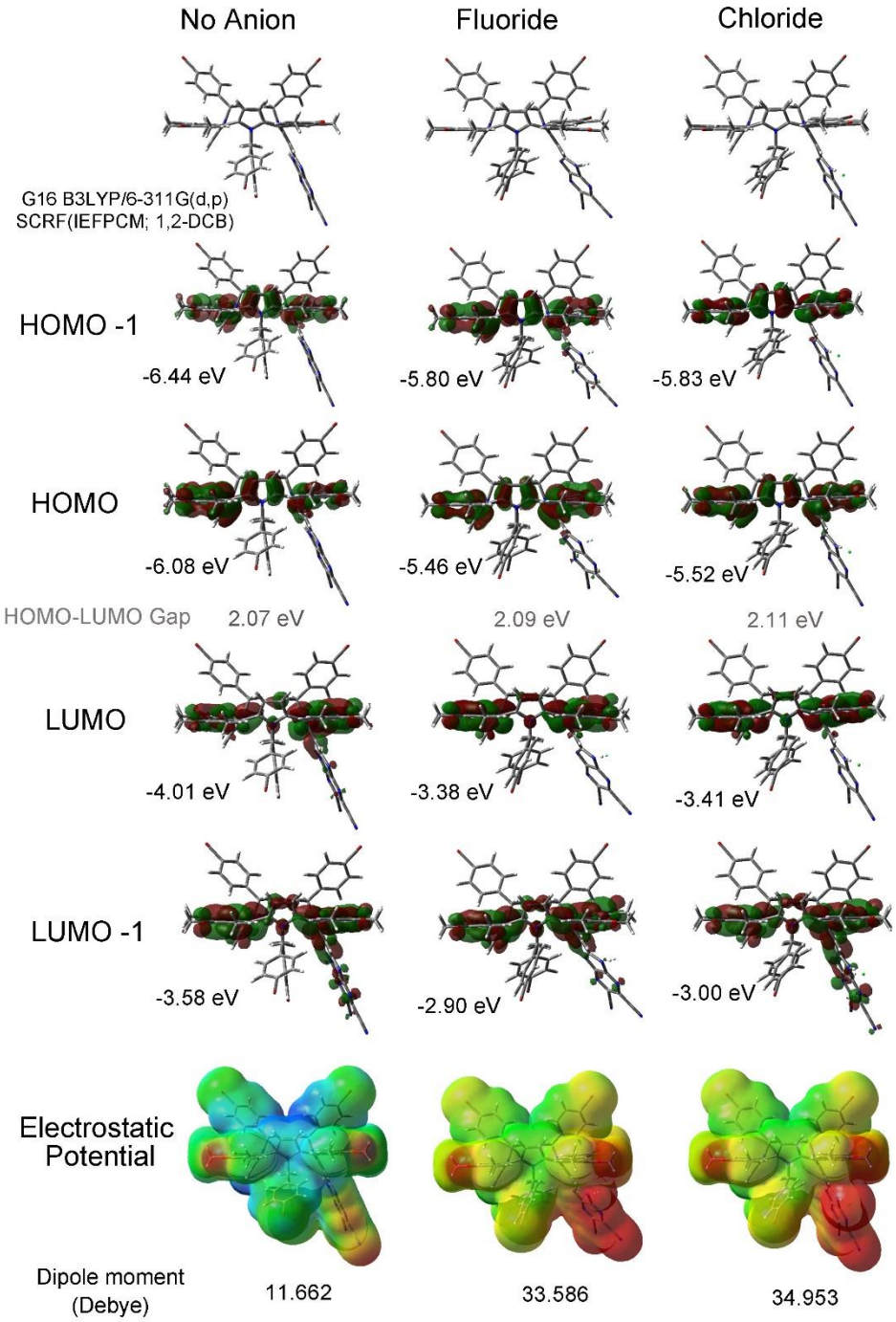

Figure S3. Calculated structures of **2**. Structures of the HOMO and LUMO orbitals in the absence and presence of fluoride or chloride anions revealing only minor perturbations by interaction of the anions at β-substituent. The main effect is global increase in energy level of the orbitals without significant variation of the HOMO-LUMO gap. Substantial increases in dipole moment suggest increasing ionic character apparently at the β-substituent.

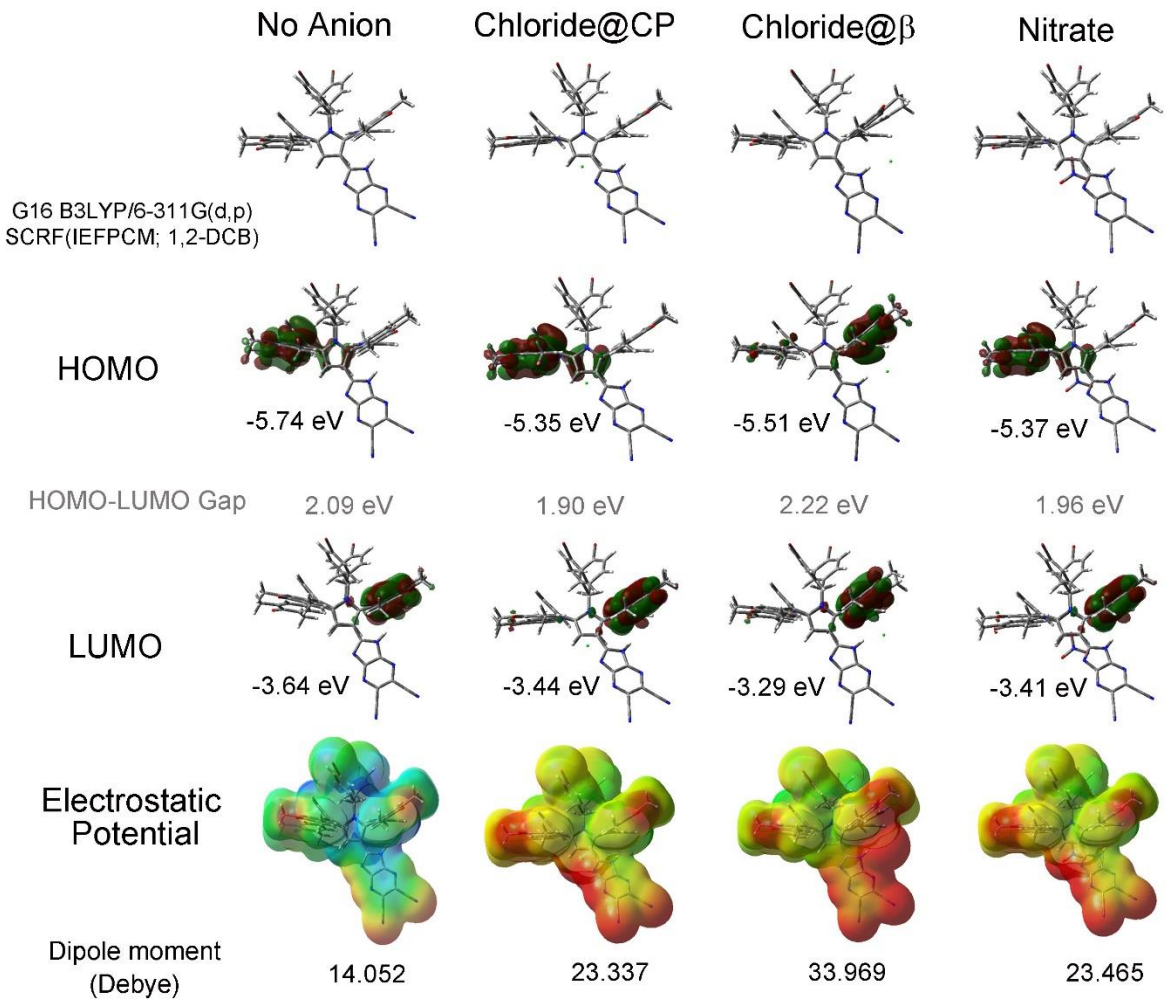

Figure S4. Calculated structures of **1**. Structures of the HOMO and LUMO orbitals in the absence and presence of anions suggest that binding at calix[4]pyrrole closes somewhat the HOMO-LUMO gap, while binding at β-substituent opens it slightly. Interaction at the β-substituent increases the dipole moment (similarly to **2**) more substantially than interaction at calix[4]pyrrole.

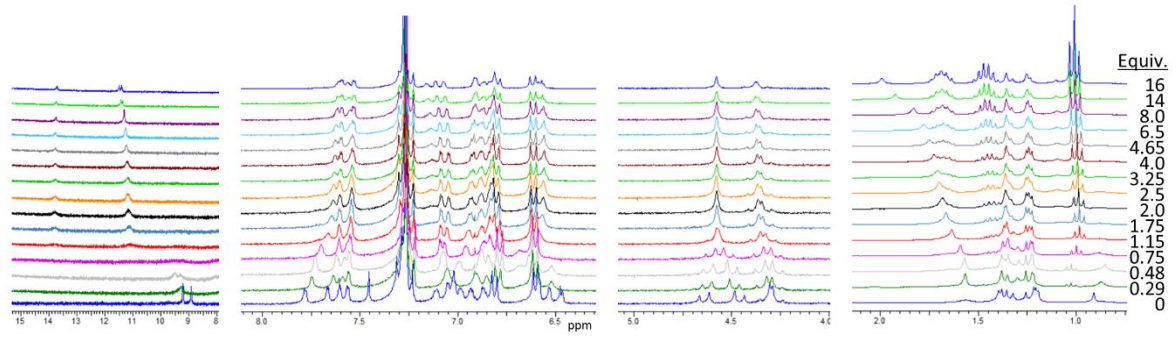

Figure S5. ^{1}H NMR spectra of **1** (2.23 mM, 25 °C) during the titration with TBACl. Number of equiv. are denoted at each spectrum as a ratio of salt guest to host concentration. For complete spectral assignment see Figure S1.

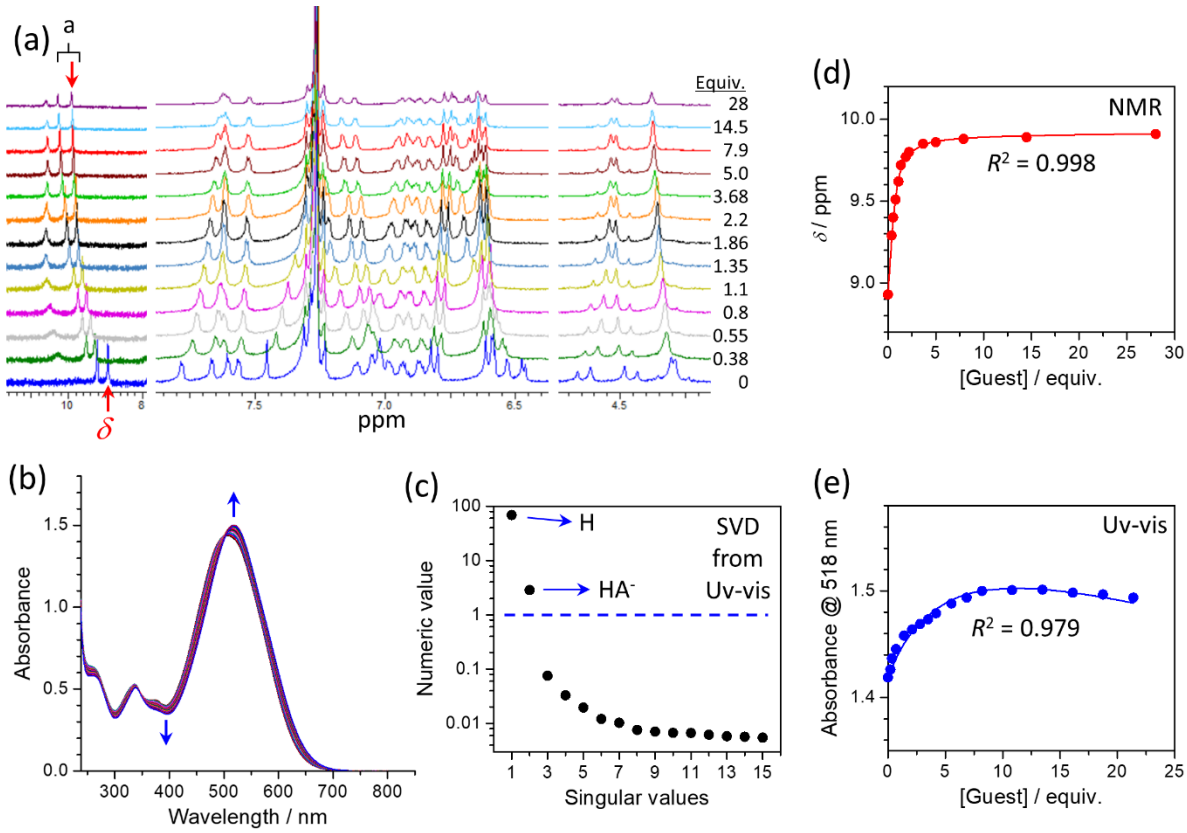

Figure S6. (a) Partial ^{1}H NMR spectra of **1** (2.23×10^{-3} M, $CDCl_3$, 25 °C) during the titration with $TBAClO_4$ (no. of equiv. is denoted at each spectrum). (b) UV-vis spectra of **1** (1.46×10^{-5} M, CH_2Cl_2, 25 °C) during the titration with 0-21 equiv. $TBAClO_4$. (c) Singular values as obtained from SVD decomposition of titration in (b) indicate only two significant components (species). (d, e) Experimental binding isotherms (solid circles) as constructed from NMR (resonance at 8.9 ppm) and UV-vis (abs. at 518 nm) titration experiments. Theoretical binding isotherms (solid lines) were constructed from model described in the text and were fitted simultaneously.

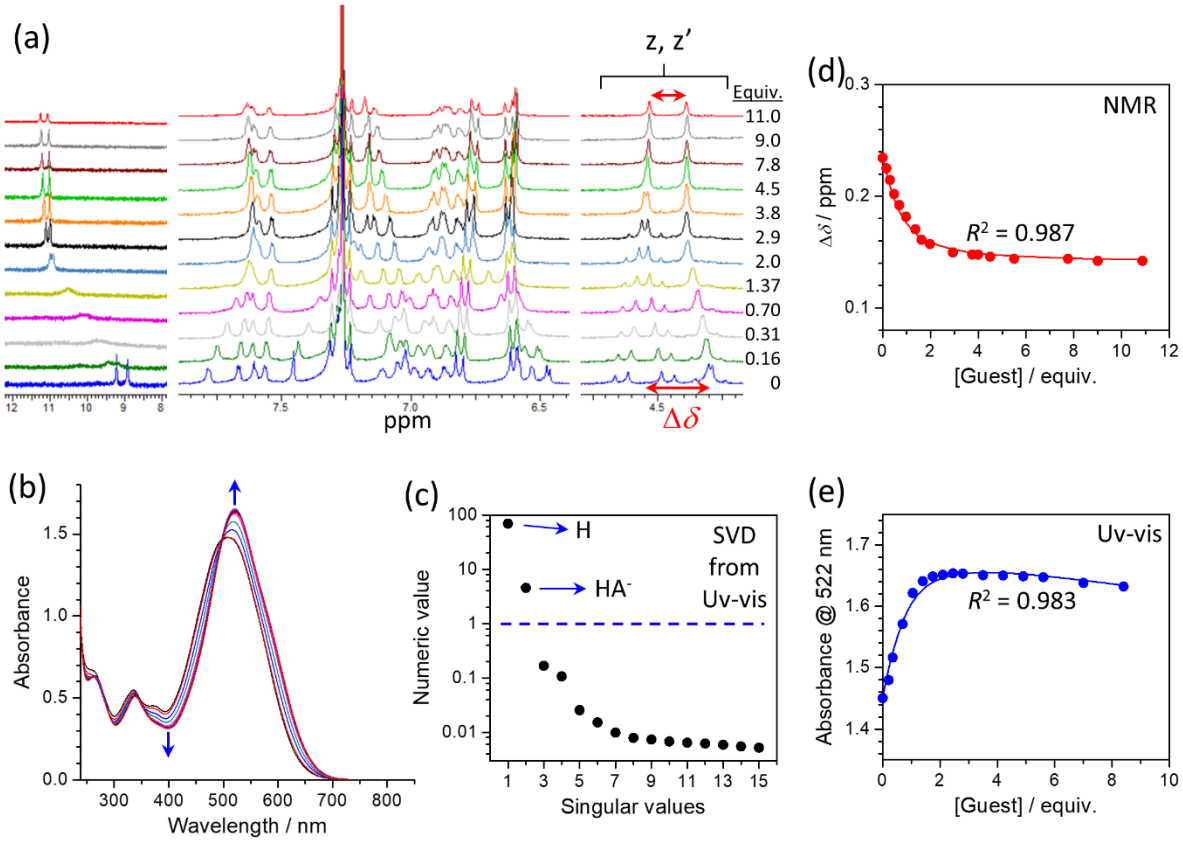

Figure S7. (a) Partial ^{1}H NMR spectra of **1** (2.23×10^{-3} M, $CDCl_3$, 25 °C) during the titration with $TBAHSO_4$ (no. of equiv. is denoted at each spectrum). (b) UV-vis spectra of **1** (1.46×10^{-5} M, CH_2Cl_2, 25 °C) during the titration with 0-8.4 equiv. $TBAHSO_4$. (c) Singular values as obtained from SVD decomposition of titration in (b) indicate only two significant components (species). (d, e) Experimental binding isotherms (solid circles) as constructed from NMR (the difference between centers of two resonance at around 4.5 ppm) and UV-vis (abs. at 522 nm) titration experiments. Theoretical binding isotherms (solid lines) were constructed from model described in the text and were fitted simultaneously.

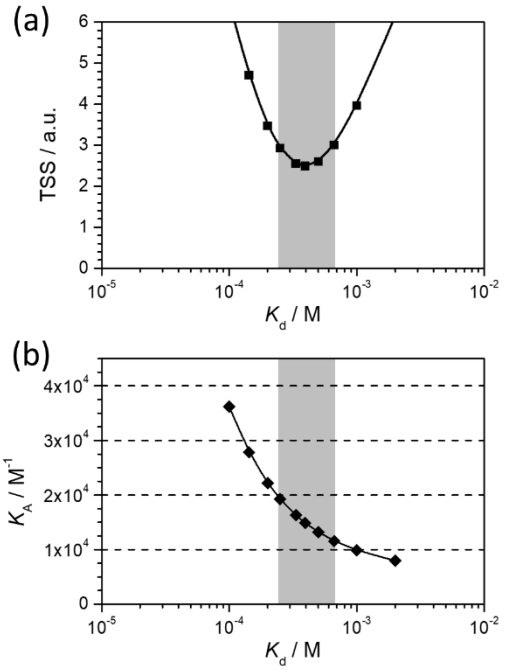

Figure S8. Result of the simultaneous NMR and UV-vis data fitting analysis of **1** with $TBAClO_4$ with variable K_d. (a) Plot of total sum of squares (TSS) dependence on K_d of $TBAClO_4$. (b) Plot of K_A dependence on K_d. Gray regions denotes acceptable TSS values.

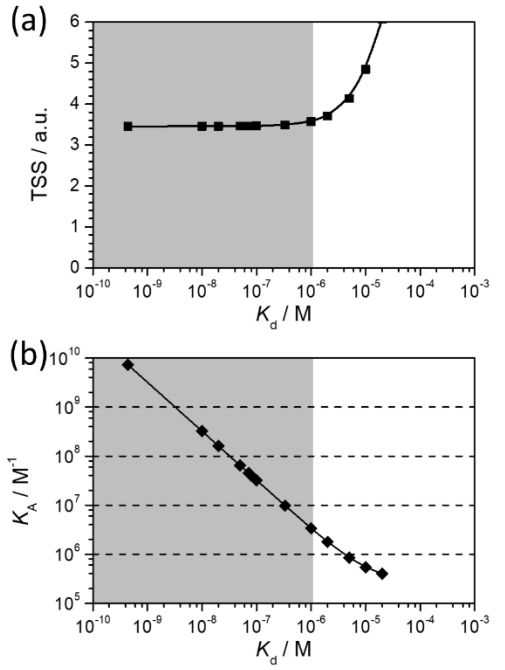

Figure S9. Result of the simultaneous NMR and UV-vis data fitting analysis of **1** with $TBAHSO_4$ with variable K_d. (a) Plot of total sum of squares (TSS) dependence on K_d of $TBAHSO_4$. (b) Plot of K_A dependence on K_d. Gray regions denotes acceptable TSS values.

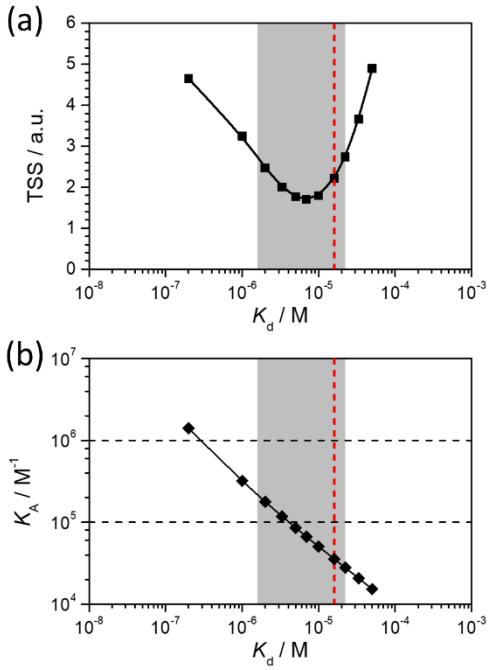

Figure S10. Result of the simultaneous NMR and UV-vis data fitting analysis of Bn_2OxP with TBACl with variable K_d. (a) Plot of total sum of squares (TSS) dependence on K_d of TBACl. (b) Plot of K_A dependence on K_d. Red dashed lines in (a,b) indicate value of TBACl dissociation constant in CH_2Cl_2 (K_d = 1.6×10^{-5} M).[S1] Gray regions denotes acceptable TSS values.

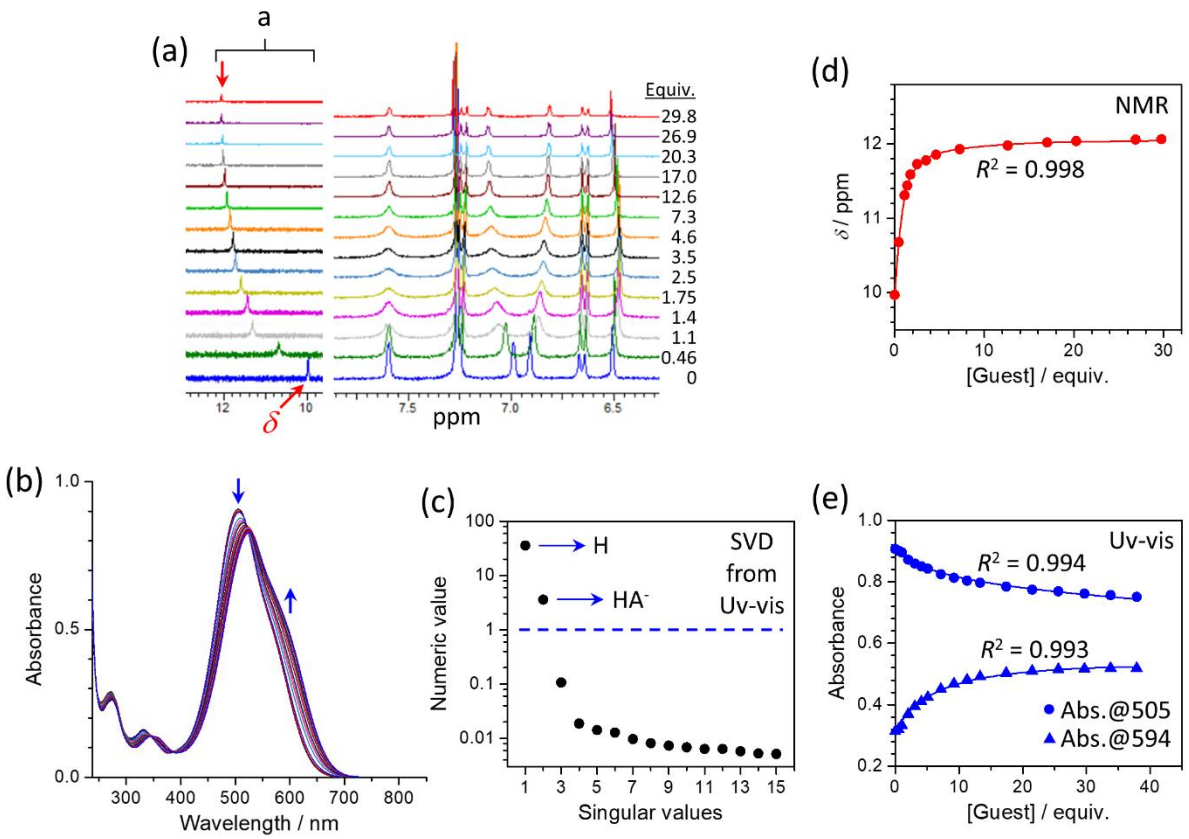

Figure S11. (a) Partial ^{1}H NMR spectra of Bn_2OxP (2.79×10^{-3} M, $CDCl_3$, 25 °C) during the titration with $TBANO_3$ (no. of equiv. is denoted at each spectrum). (b) UV-vis spectra of Bn_2OxP (6.15×10^{-6} M, CH_2Cl_2, 25 °C) during the titration with 0-38 equiv. $TBANO_3$. (c) Singular values as obtained from SVD decomposition of titration in (b) indicate only two significant components (species). (d, e) Experimental binding isotherms (solid circles) as constructed from NMR (resonance at 10 ppm) and UV-vis (abs. at 505 nm and 594 nm) titration experiments. Theoretical binding isotherms (solid lines) were constructed from model described in the text and were fitted simultaneously.

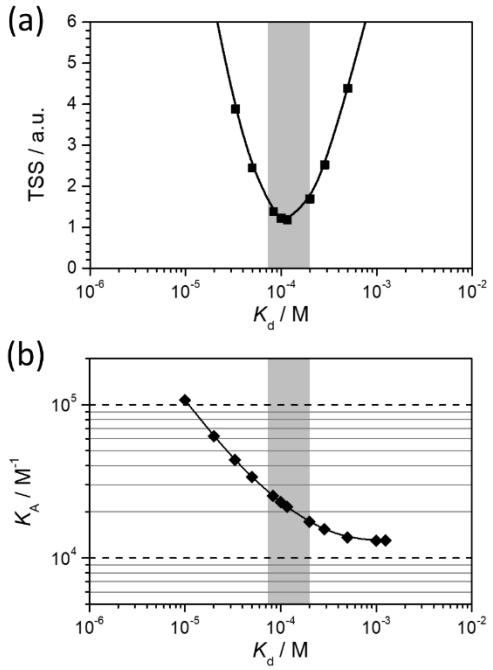

Figure S12. Result of the simultaneous NMR and UV-vis data fitting analysis of Bn_2OxP with $TBANO_3$ with variable K_d. (a) Plot of total sum of squares (TSS) dependence on K_d of $TBANO_3$. (b) Plot of K_A dependence on K_d. Gray regions denotes acceptable TSS values.

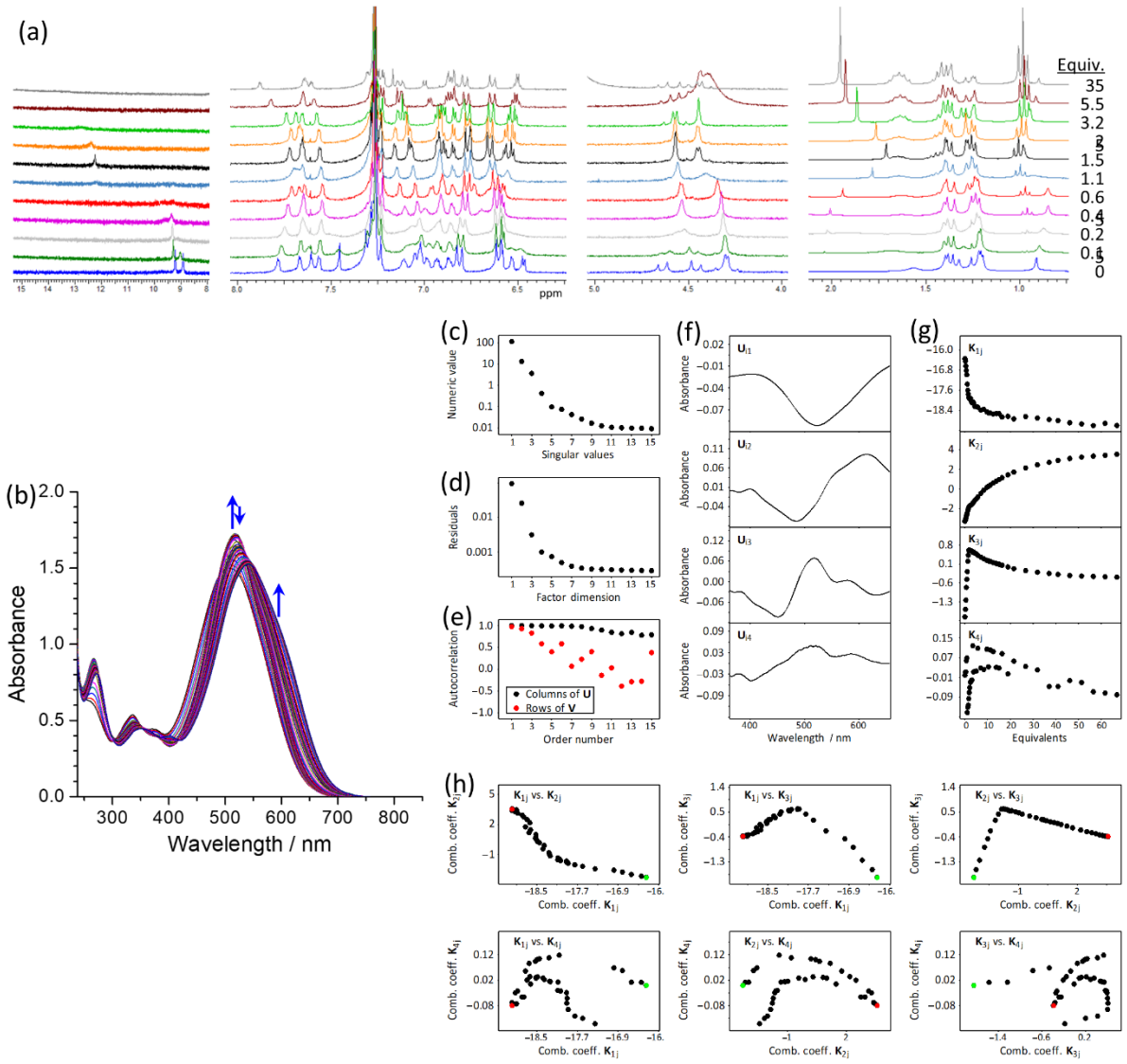

Figure S13. (a) ^{1}H NMR spectra of **1** (2.23 mM, $CDCl_3$, 25 °C) during the titration with TBAOAc. Number of equiv. are denoted at each spectrum. (b) UV-vis spectra of **1** (1.46×10^{-5} M, CH_2Cl_2, 25 °C) during the titration with 0-67 equiv. TBAOAc. (c-h) SVD decomposition of UV-vis titration from (b). (c) Singular values indicating the presence of at least three components (species). (d) Residuals. (e) Autocorrelations of basis **U** and amplitude vectors **V**, respectively. (f) First four basis vectors **U**. (g) First four amplitude vectors **V**. (h) Mutual dependence of first three combination coefficients (red and green dots denote first and last measured spectrum, respectively).

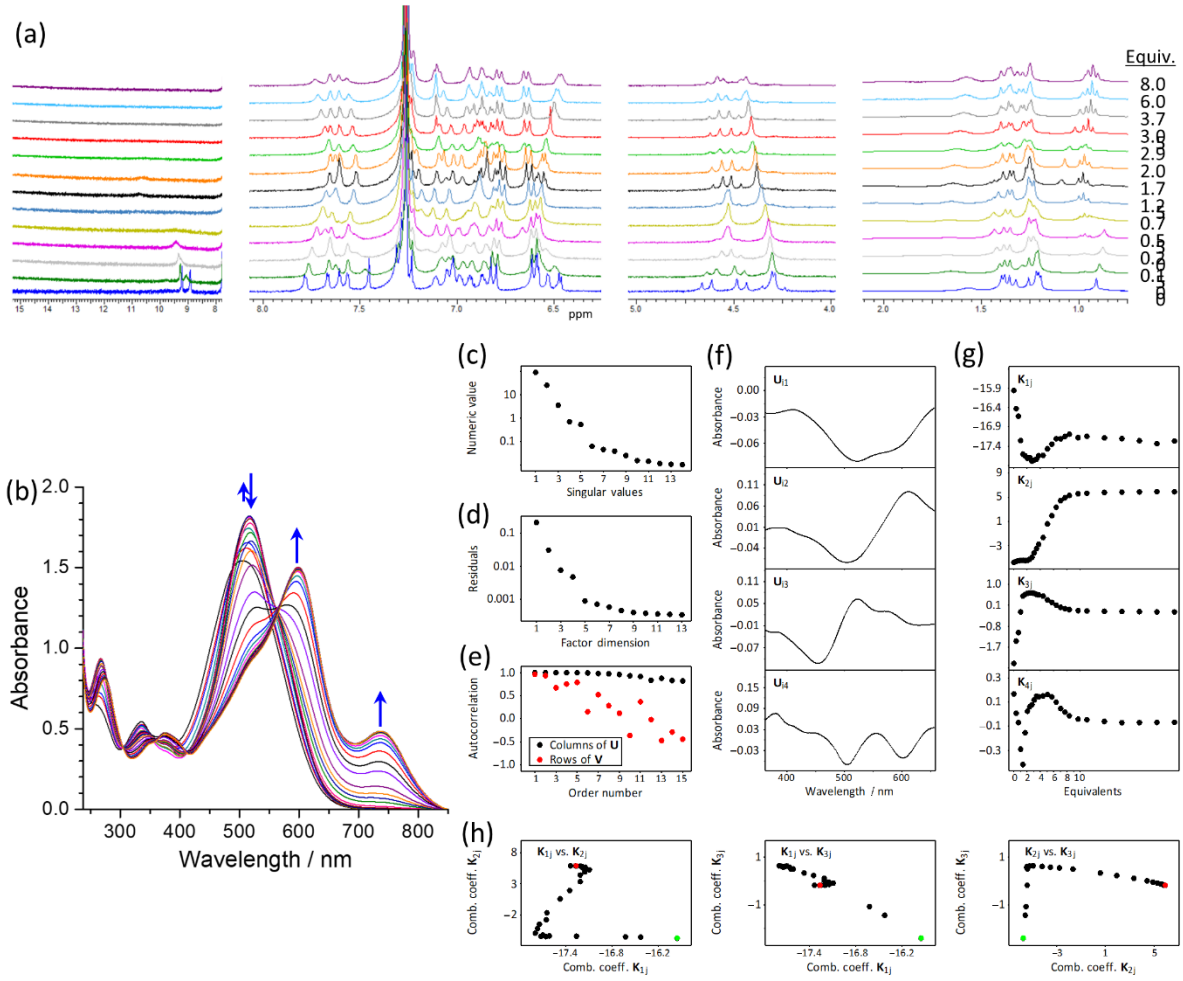

Figure S14. (a) ^{1}H NMR spectra of **1** (2.23 mM, $CDCl_3$, 25 °C) during the titration with TBAF. Number of equiv. are denoted at each spectrum. (b) UV-vis spectra of **1** (1.46×10^{-5} M, CH_2Cl_2, 25 °C) during the titration with 0-24 equiv. TBAF. (c-h) SVD decomposition of UV-vis titration from (b). (c) Singular values indicating the presence of at least three components (species). (d) Residuals. (e) Autocorrelations of basis **U** and amplitude vectors **V**, respectively. (f) First four basis vectors **U**. (g) First four amplitude vectors **V**. (h) Mutual dependence of first three combination coefficients (red and green dots denote first and last measured spectrum, respectively).

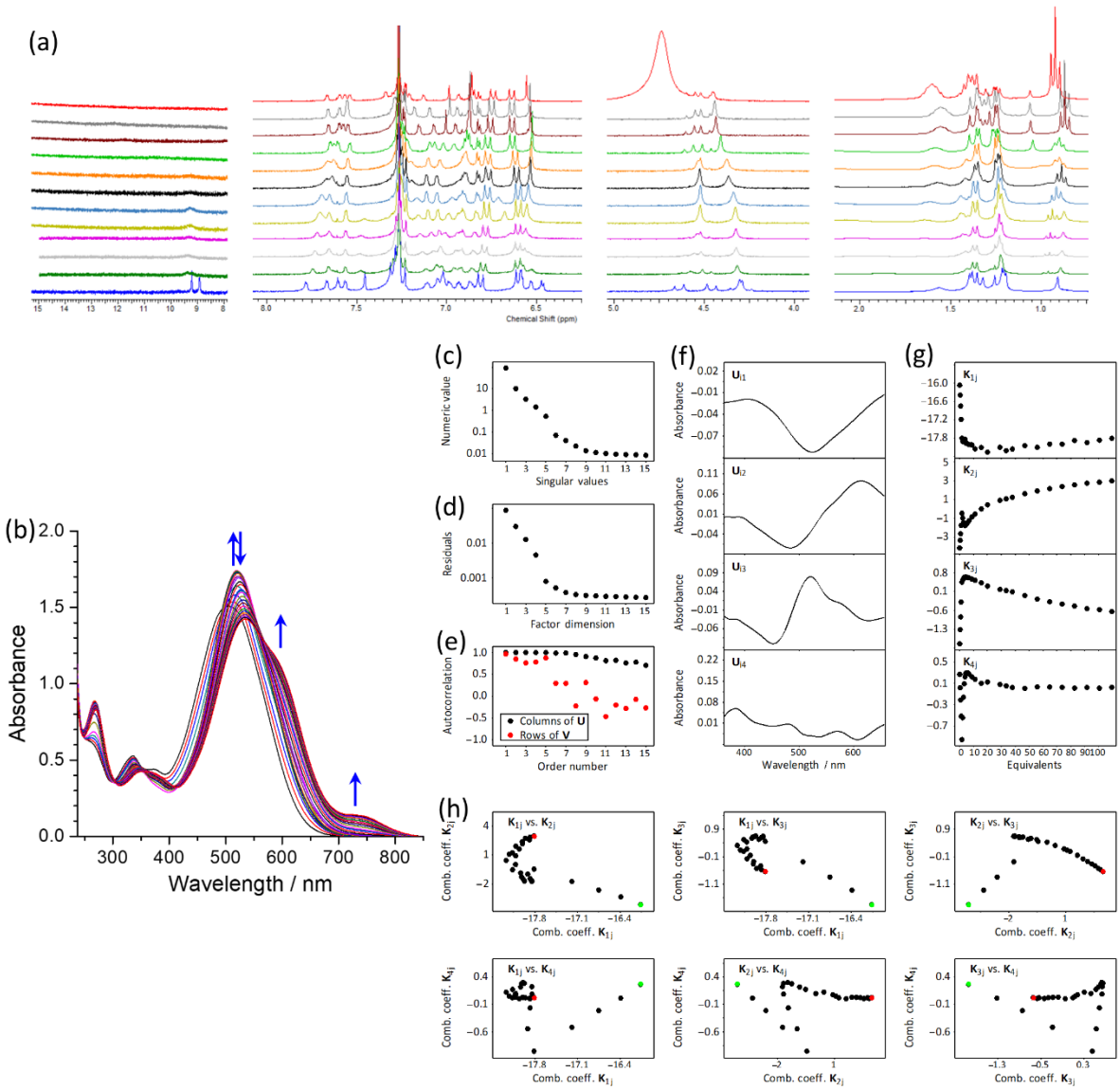

Figure S15. (a) ^{1}H NMR spectra of **1** (2.23 mM, $CDCl_3$, 25 °C) during the titration with 0-16 equiv. $TBAH_2PO_4$ (bottom spectrum = neat host). (b) UV-vis spectra of **1** (1.46×10^{-5} M, CH_2Cl_2, 25 °C) during the titration with 0-110 equiv. $TBAH_2PO_4$. (c-h) SVD decomposition of UV-vis titration from (b). (c) Singular values indicating the presence of at least four components (species). (d) Residuals. (e) Autocorrelations of basis **U** and amplitude vectors **V**, respectively. (f) First four basis vectors **U**. (g) First four amplitude vectors **V**. (h) Mutual dependence of first three combination coefficients (red and green dots denote first and last measured spectrum, respectively).

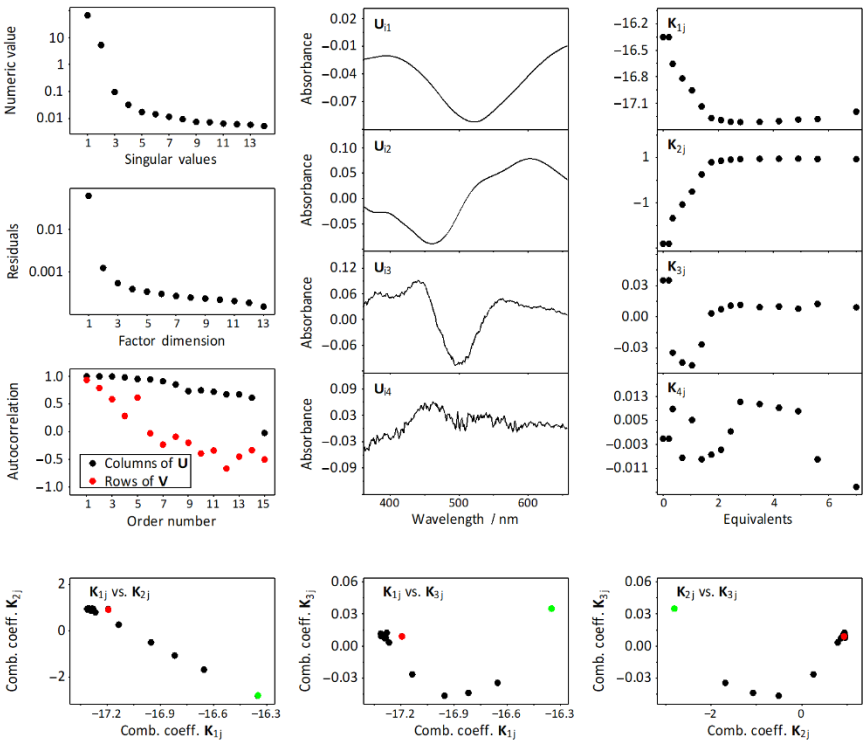

Figure S16. SVD decomposition of titration of **1** with TBACl in CH_2Cl_2. For actual UV-vis spectra see Figure 4 in the main manuscript. (a) Singular values indicating the presence of only two species, i.e. free host (H) and anion-host complex (HA^-). (b) Residuals (significant drop can be seen at factor dimension = 2). (c) Autocorrelations of basis **U** and amplitude vectors **V**, respectively. (d) First four basis vectors **U**. (e) First four amplitude vectors **V**. (f) Mutual dependence of first three combination coefficients (red and green dots denote first and last measured spectrum, respectively).

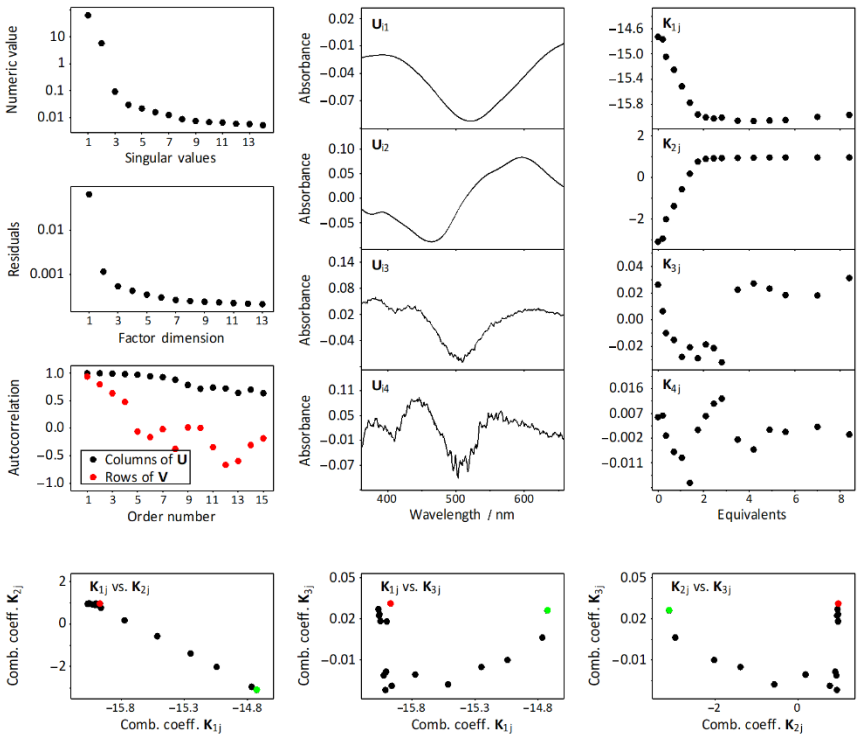

Figure S17. SVD decomposition of titration of **1** with $TBANO_3$ in CH_2Cl_2. For actual UV-vis spectra see Figure 5 in the main manuscript. (a) Singular values indicating the presence of only two species, i.e. free host (H) and anion-host complex (HA^-). (b) Residuals (significant drop can be seen at factor dimension = 2). (c) Autocorrelations of basis **U** and amplitude vectors **V**, respectively. (d) First four basis vectors **U**. (e) First four amplitude vectors **V**. (f) Mutual dependence of first three combination coefficients (red and green dots denote first and last measured spectrum, respectively).

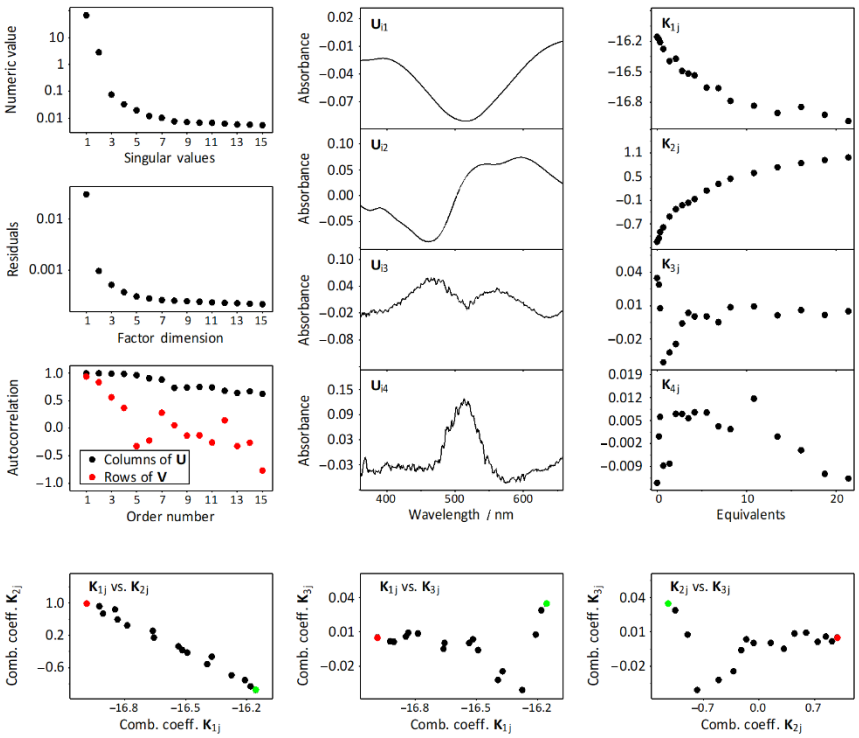

Figure S18. SVD decomposition of titration of **1** with $TBAClO_4$ in CH_2Cl_2. For actual UV-vis spectra see Figure S6. (a) Singular values indicating the presence of only two species, i.e. free host (H) and anion-host complex (HA^-). (b) Residuals (significant drop can be seen at factor dimension = 2). (c) Autocorrelations of basis **U** and amplitude vectors **V**, respectively. (d) First four basis vectors **U**. (e) First four amplitude vectors **V**. (f) Mutual dependence of first three combination coefficients (red and green dots denote first and last measured spectrum, respectively).

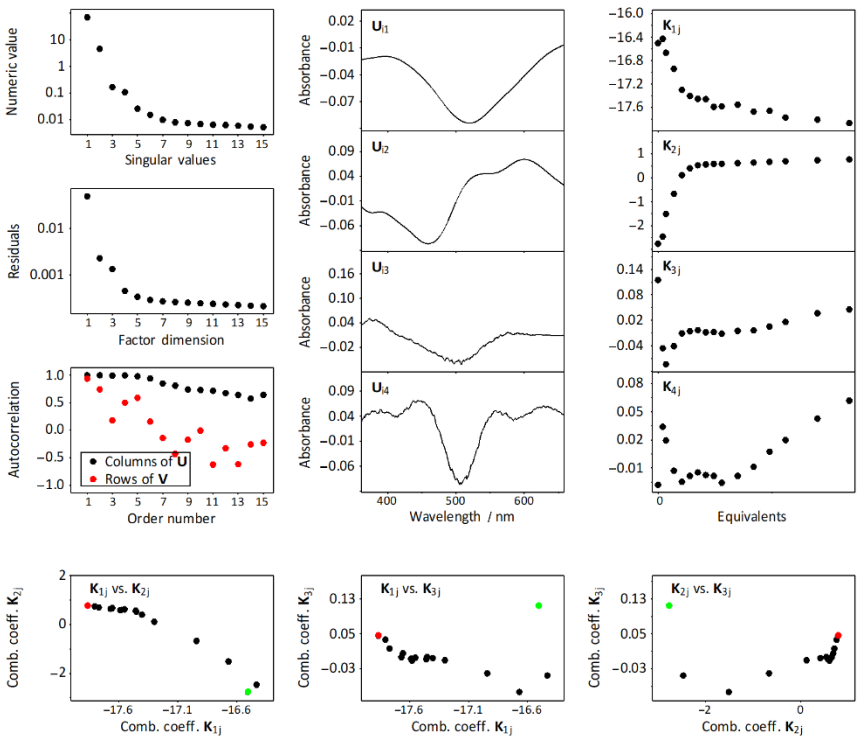

Figure S19. SVD decomposition of titration of **1** with $TBAHSO_4$ in CH_2Cl_2. For actual UV-vis spectra see Figure S7. (a) Singular values indicating the presence of only two species, i.e. free host (H) and anion-host complex (HA^-). (b) Residuals (significant drop can be seen at factor dimension = 2). (c) Autocorrelations of basis **U** and amplitude vectors **V**, respectively. (d) First four basis vectors **U**. (e) First four amplitude vectors **V**. (f) Mutual dependence of first three combination coefficients (red and green dots denote first and last measured spectrum, respectively).

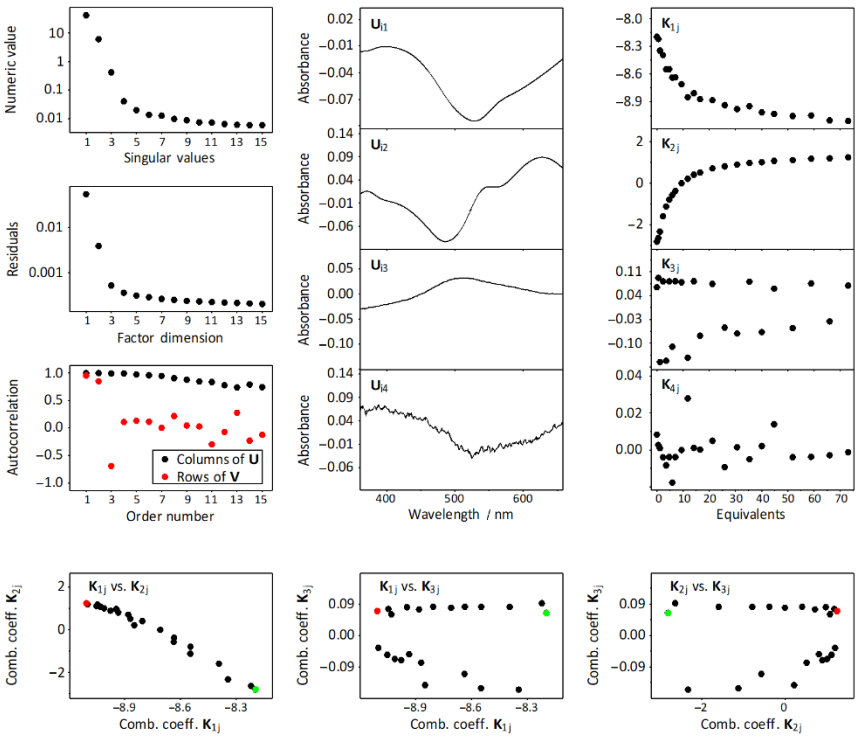

Figure S20. SVD decomposition of titration of Bn_2OxP with TBACl in CH_2Cl_2. For actual UV-vis spectra see Figure 10 in the main manuscript. (a) Singular values indicating the presence of only two species, i.e. free host (H) and anion-host complex (HA^-). (b) Residuals (significant drop can be seen at factor dimension = 2). (c) Autocorrelations of basis **U** and amplitude vectors **V**, respectively. (d) First four basis vectors **U**. (e) First four amplitude vectors **V**. (f) Mutual dependence of first three combination coefficients (red and green dots denote first and last measured spectrum, respectively).

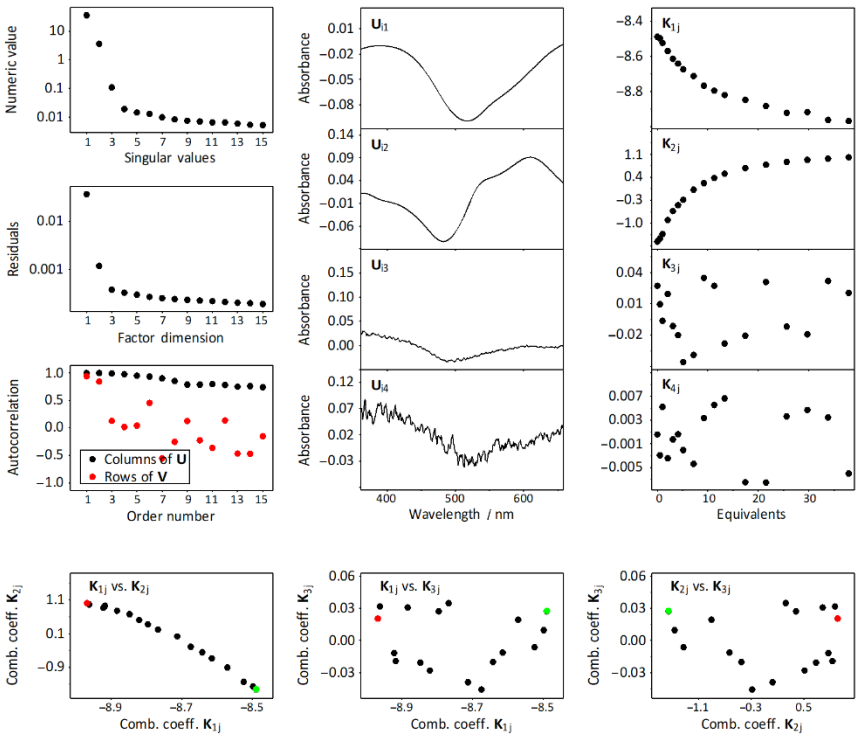

Figure S21. SVD decomposition of titration of Bn_2OxP with $TBANO_3$ in CH_2Cl_2. For actual UV-vis spectra see Figure S11. (a) Singular values indicating the presence of only two species, i.e. free host (H) and anion-host complex (HA^-). (b) Residuals (significant drop can be seen at factor dimension = 2). (c) Autocorrelations of basis **U** and amplitude vectors **V**, respectively. (d) First four basis vectors **U**. (e) First four amplitude vectors **V**. (f) Mutual dependence of first three combination coefficients (red and green dots denote first and last measured spectrum, respectively).

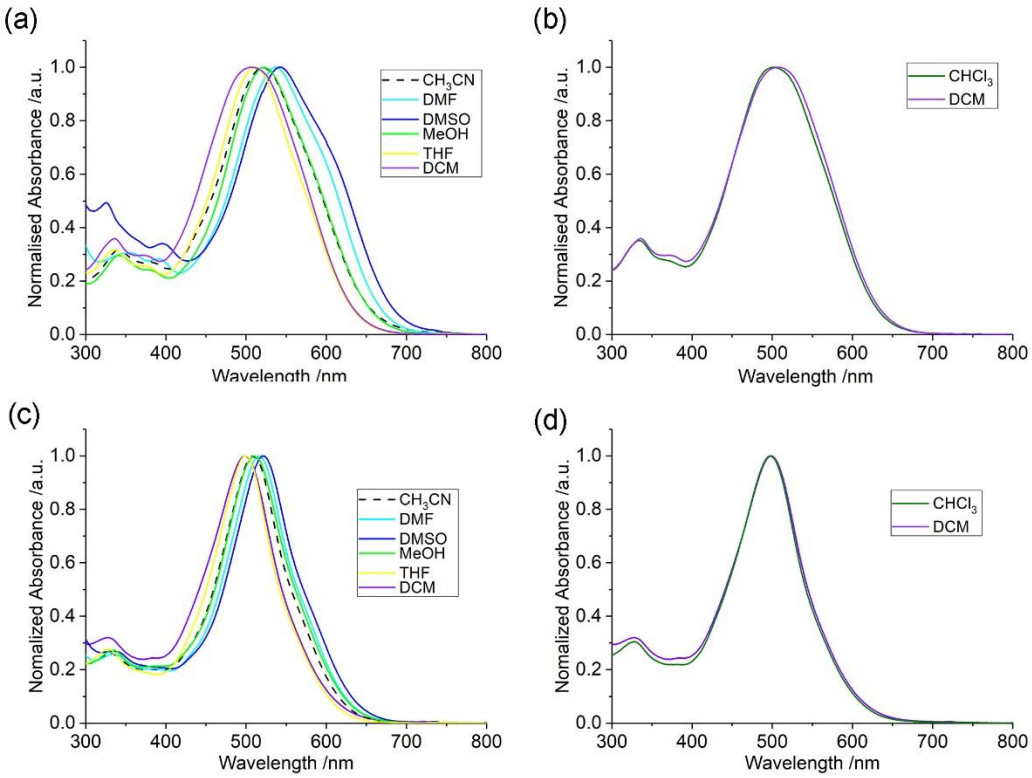

Figure S22. Electronic absorption spectra of **1** and **2** in different solvents revealing bathochromic shifts caused by increasing solvent polarity (CH_3CN: acetonitrile; DMF: N,N-dimethylformamide; DMSO: dimethylsulphoxide; MeOH: methanol; THF: tetrahydrofuran; DCM: dichloromethane). (a) **1** in solvents of different polarity. (b) Electronic absorption spectra of **1** in DCM or $CHCl_3$ revealing the marginal difference in spectrum between the two solvents. (c) **2** in solvents of different polarity. (d) Electronic absorption spectra of **2** in DCM or $CHCl_3$ revealing the marginal difference in spectrum between the two solvents. The increasing hydrogen bond acceptor character of the solvent shifts the absorption maximum by up to ~50 nm and 25 nm for **1** and **2**, respectively.

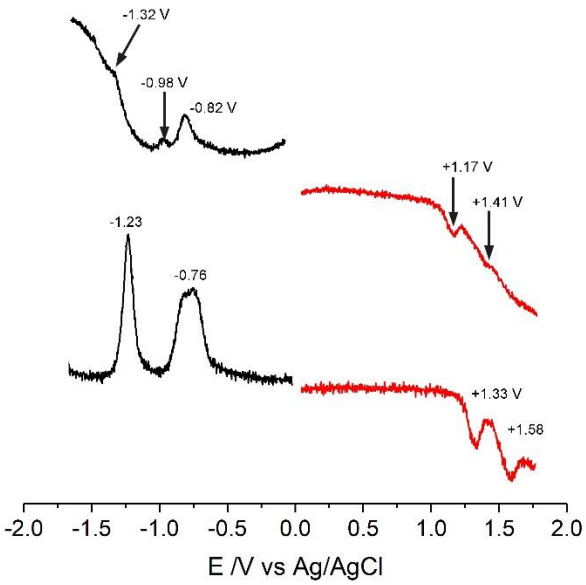

Figure S23. Differential pulsed voltammetry for compounds **1** (upper) and **2** (lower). Oxidation and reduction potentials are similar to those found for unsubstituted macrocycles Bn_2OxP and Bn_4OxP, respectively.[S8]

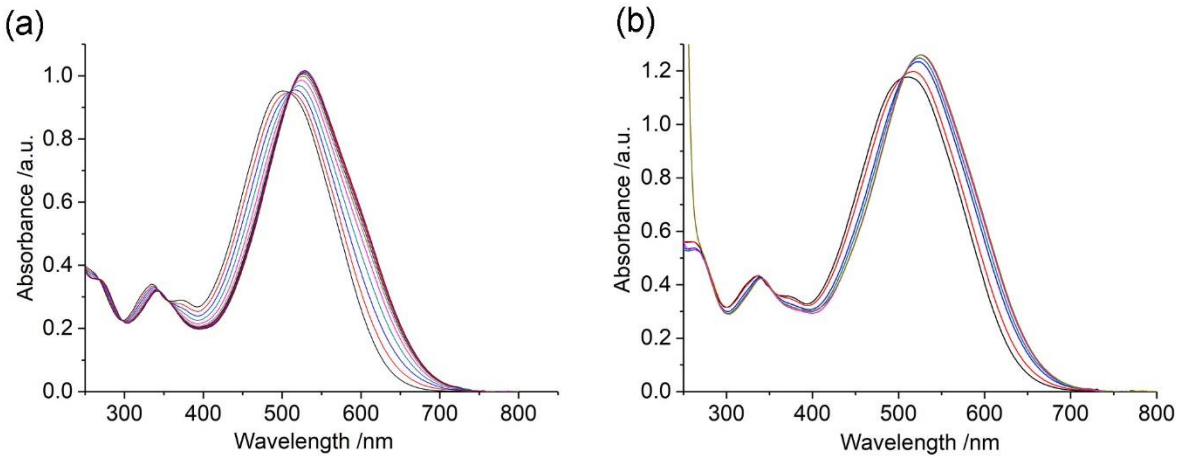

Figure S24. Qualitative responses of host **1** to (a) bromide anions and (b) thiocyanate anions. Aliquots of the respective anions in CH_2Cl_2 were added to solutions of **1** in CH_2Cl_2 until the response was saturated.

Synthesis

2-Formyl-5,10,15,20-tetrakis(3,5-di-*tert*-butyl-4-oxo-cyclohexa-2,5-dienylidene)porphyrinogen, OxP-CHO.

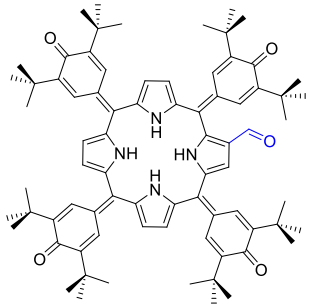

Vilsmeier reagent was prepared by adding phosphoryl chloride (8.12 g, 52.9 mmol, 63.0 equiv.) to DMF (5.96 g, 81.5 mmol, 97.0 equiv.) at 0 °C under nitrogen followed by stirring for 10 minutes. [T(DtBHP)P]Cu[S9] (1 g, 0.84 mmol, 1.0 equiv.) in dichloromethane (30 mL) was added and the reaction was heated at reflux for 18 hours. The resulting reaction mixture was cooled to 0 °C and conc. H_2SO_4 (~6 mL) was added dropwise followed by stirring until complete demetallation had occurred (organic layer turns colourless once demetallation is complete). The resulting solution was poured carefully into 3M NaOH solution (400 mL) over crushed ice and extracted with dichloromethane (3 x 100 mL). The organic fractions were combined, dried over anhydrous sodium sulfate and the solvent was removed under reduced pressure. The solid was redissolved into dichloromethane (100 mL) and tetrabutylammonium hydroxide solution (0.5 mL, 1.0 M in methanol) was added and stirred for 30 minutes. The resulting mixture was washed with water (200 mL), dried over anhydrous sodium sulfate and passed through a plug of silica (dichloromethane/acetone 9:1) to give **OxP-CHO** as a dark olive green solid (0.9 g, 93%). Note: ^{1}H and ^{13}C NMR spectra could not be obtained due to the low solubility of this compound. FT-IR(KBr): ν = 3438.9 (w), 3179.0 (w), 2999.7 (w), 2952.1 (m), 2919.2 (m), 2862.9 (w), 1638.4 (m), 1605.3 (s), 1563.0 (s), 1485.1 (m), 1453.3 (s), 1388.0 (w), 1361.5 (s), 1340.7 (w), 1297.7 (m), 1264.1 (m), 1088.8 (m), 1027.6 (m), 997.2 (w), 939.5 (w), 929.5 (w), 885.9 (w), 834.6 (w), 819.1 (w), 802.0 (w) cm^{-1}; MALDI-TOF-MS (dithranol): calc'd for $[C_{77}H_{94}N_4O_5]^+$ = 1154.72; found: $[C_{77}H_{94}N_4O_5]^+$ = 1154.19 ($[M + 2H]^+$); UV/Vis (CH_2Cl_2): 337 and 506 (λ_{max}) nm.

N_{21},N_{23}-Bis(4-bromobenzyl)-2-formyl-5,10,15,20-tetrakis(3,5-di-*tert*-butyl-4-oxo-cyclohexa-2,5-dienylidene) porphyrinogen (Bn_2OxP-CHO) and **N_{21},N_{22},N_{23},N_{24}-tetrakis(4-bromobenzyl)-2-formyl-5,10,15,20-tetrakis(3,5-di-*tert*-butyl-4-oxo-cyclohexa-2,5-dienylidene)porphyrinogen (Bn_4OxP-CHO).**

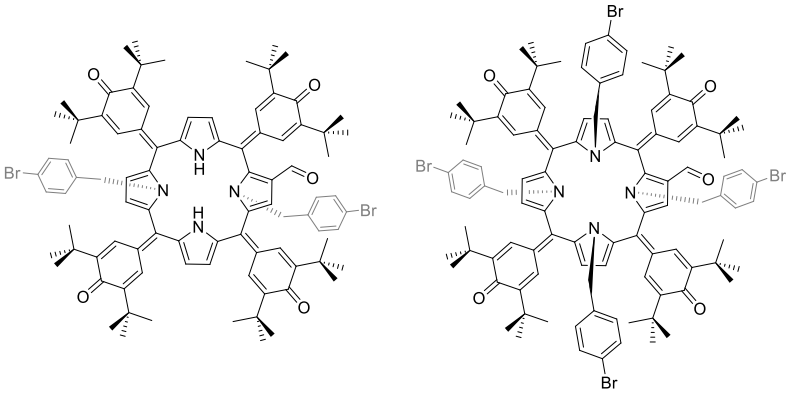

Alkylation of **OxP-CHO** was carried out according to a literature procedure.[S8] 4-Bromobenzyl bromide (260 mg, 1.04 mmol, 4.0 equiv.) and sodium carbonate (1.10 g, 10.4 mmol, 40.0 equiv.) were added to **OxP-CHO** (300 mg, 0.26 mmol, 1.0 equiv.) in acetone (30 mL) and heated to reflux for 5 hours, after which a further aliquot of 4-bromobenzyl bromide (195 mg, 0.78 mmol, 3.3 equiv.) was added whilst the temperature was maintained. The reaction was monitored by thin layer chromatography until complete consumption of **OxP-CHO** was observed. The reaction solvent was removed under reduced pressure and the residue was partitioned between water (20 mL) and dichloromethane (30 mL), the phases were separated and the organic phase was dried over anhydrous sodium sulfate, filtered and the solvent was removed under reduced pressure. The residue was purified by column chromatography (SiO_2), elution with dichloromethane gave **Bn_4OxP-CHO** as a red solid (Yield: 50 mg, 10%) followed by elution of **Bn_2OxP-CHO** as a greenish solid (Yield: 274 mg, 70%) with dichloromethane/acetone (99:1, v/v). *Note: The tetra-N-alkylated product can be obtained as the major product (>90%) under modified conditions using >10 equiv. of 4-bromobenzyl bromide heating at reflux for 2-3 days.*

Bn_2OxP-CHO: ^{1}H NMR (300 MHz, $CDCl_3$/acetone-d_6): δ = 10.81 (s, 1H), 10.68 (s, 1H), 9.34 (s, 1H, -CHO), 7.60-7.79 (m, 4H), 7.24-7.30 (m, 4H), 6.90-7.10 (m, 8H), 6.64-6.81 (m, 5H), 6.48 (s, 2H), 4.38-4.60 (m, 4H), 1.15-1.39 (m, 72H) ppm; ^{13}C NMR (76 MHz, $CDCl_3$/acetone-d_6): δ = 186.1, 185.2, 150.0, 149.2, 148.6, 147.8, 141.3, 136.8, 136.3, 135.9, 135.6, 135.5, 135.3, 135.1, 134.8, 133.3, 132.6, 132.2, 132.2, 132.0, 131.9, 131.7, 130.8, 130.7, 130.6, 130.1, 130.0, 129.4, 129.3, 128.9, 128.8, 126.2, 122.9, 122.4, 120.2, 120.0, 116.9, 48.9, 48.7, 35.8, 35.5, 35.5, 30.7, 30.6, 30.4, 30.3, 30.1, 30.1, 29.9, 29.8, 29.6, 29.3 ppm; FT-IR(KBr): v = 3248.5 (w), 2998.2 (w), 2959.2 (m), 2864.6 (w), 1638.6 (m), 1605.9 (s), 1596.2 (s), 1564.7 (w), 1527.7

(w), 1488.8 (m), 1455.0 (m), 1407.3 (w), 1389.4 (w), 1361.3 (m), 1333.9 (w), 1320.6 (w), 1295.9 (w), 1266.6 (w), 1156.0 (m), 1085.8 (m), 1072.8 (m), 1028.3 (m), 1012.1 (w), 982.1 (w), 949.2 (w), 929.5 (w), 917.2 (w) cm^{-1}; MALDI-TOF-MS (dithranol): calc'd for $[C_{91}H_{103}Br_2N_4O_5]^+$ = 1489.62; found: $[C_{91}H_{103}Br_2N_4O_5]^+$ = 1489.62 ($[M + H]^+$); UV/Vis (CH_2Cl_2): 325 and 499 (λ_{max}) nm.

Bn_4OxP-CHO: ^{1}H NMR (300 MHz, $CDCl_3$): δ = 9.01 (s, 1H), 7.44 (d, J = 2.6 Hz, 1H), 7.29-7.33 (m, 8H), 7.12-7.24 (m, 6H), 6.78-6.83 (m, 2H), 6.74 (d, J = 3.7 Hz, 1H), 6.61-6.70 (m, 7H), 6.52-6.57 (m, 4H), 6.40-6.43 (m, 2H), 4.24-4.62 (m, 8H), 1.15-1.31 (m, 72H) ppm; ^{13}C NMR (76 MHz, $CDCl_3$/acetone-d_6): δ = 132.5, 132.4, 128.3, 128.0, 127.2, 77.7, 77.6, 77.5, 77.2, 77.2, 77.1, 76.8, 76.7, 35.8, 30.4, 30.3, 30.2, 30.1, 29.9, 29.8, 29.7, 29.6, 29.5 ppm; FT-IR(KBr): ν = 2996.8 (w), 2957.1 (m), 2919.1 (w), 2864.3 (w), 1681.8 (w), 1605.1 (s), 1526.0 (w), 1488.4 (m), 1455.2 (w), 1405.9 (w), 1388.0 (w), 1361.6 (s), 1315.6 (m), 1255.1 (w), 1086.8 (w), 1072.4 (m), 1011.0 (m), 956.5 (w), 943.4 (w), 929.2 (w), 880.5 (w), 836.5 (w), 819.2 (w) cm^{-1}; MALDI-TOF-MS (dithranol): calc'd for $[C_{105}H_{111}Br_4N_4O_5]^+$ = 1823.52; found: $[C_{105}H_{111}Br_4N_4O_5]^+$ = 1823.41 ($[M - H]^+$); UV/Vis (CH_2Cl_2): 326 and 493 (λ_{max}) nm.

2-Hydroxymethyl-*meso*-tetrakis-(3',5'-di-*tert*-butyl-4'-hydroxyphenyl)-porphyrinatocopper(II) ([T(DtBHP)PCu]-CH_2OH).

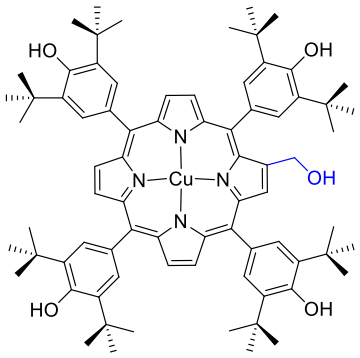

[T(DtBHP)PCu]-CHO[S9] (500 mg, 0.41 mmol) was dissolved in dry $CHCl_3$ (60 mL) and stirred for 5 minutes under N_2 atmosphere. $NaBH_4$ (280 mg, 7.40 mmol, dissolved in dry ethanol, 1 mL) was added slowly and the resulting reaction mixture was stirred overnight with ~100 % conversion of formyl-porphyrin to hydroxymethyl-porphyrin. Water was added slowly and the resulting mixture extracted with dichloromethane (100 mL), the organic extracts combined and dried over anhydrous sodium sulfate. Solvents were removed under reduced pressure yielding a purple solid, which was used in the next step without further purification.

FT-IR(ATR): ν = 3635.2 (w), 3600.3 (w), 2956.2 (m), 2870.7 (w), 1429.3 (s), 1391.0 (w), 1360.9 (w), 1344.4 (w), 1306.8 (w), 1219.5 (s), 1149.5 (m), 1119.9 (m), 1005.9 (w), 940.9 (w), 889.3 (w), 823.2 (w), 799.7 (m), 753.0 (m), 723.5 (w), 683.4 (w) cm^{-1}; MALDI-TOF-MS (dithranol): calc'd for $[C_{77}H_{94}CuN_4O_5]^+$ = 1217.65; found: $[C_{77}H_{94}CuN_4O_5]^+$ = 1215.49 ($[M - 2H]^+$); UV/Vis (CH_2Cl_2): 421 (λ_{max}), 543, 582 nm.

2-Hydroxymethyl-5,10,15,20-tetrakis(3,5-di-*tert*-butyl-4-oxo-cyclohexa-2,5-dienylidene) porphyrinogen, OxP-CH_2OH.

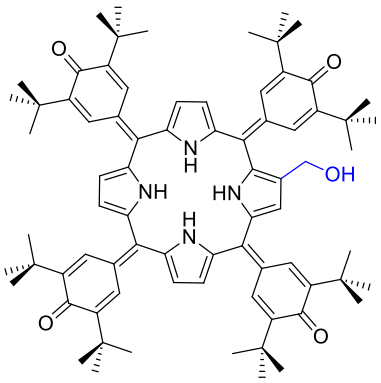

[T(DtBHP)PCu]-CH_2OH (300 mg, 0.25 mmol) was dissolved in the minimum amount of $CHCl_3$ (10 mL) and cooled to 0 °C. Concentrated H_2SO_4 (~2 mL) was added very slowly dropwise with vigorous stirring at 0 °C for 10 minutes until complete demetallation had occurred. At the end of this period, water (40 mL) was added. The organic layer was partitioned and washed with 25% aqueous ammonia solution (10 mL). The organic fraction was separated, dried over anhydrous Na_2SO_4 followed by filtration and removal of solvents under reduced pressure. The resulting solid (2-hydroxymethyl-5,10,15,20-tetrakis(3,5-di-*t*-butyl-4-hydroxyphenyl)porphyrin) was subjected to oxidation by using a literature procedure.[S3] **OxP-CH_2OH** was purified using column chromatography (SiO_2, $CHCl_3$/acetone, 99:1, v/v). The combined yield of the two steps was 54 % (154 mg).
^{1}H NMR (300 MHz, $CDCl_3$): δ = 9.52 (s, 1H), 9.13 (s, 1H), 8.81 (s, 1H), 8.71 (s, 1H), 7.57 (d, J = 2.2 Hz, 1H), 7.40-7.49 (m, 6H), 6.94 (d, J = 2.2 Hz, 1H), 6.75-6.82 (m, 7H), 4.32 (d, J = 11.4 Hz, 1H), 4.07 (d, J = 11.4 Hz, 1H), 1.29-1.35 (m, 72H) ppm; ^{13}C NMR (76 MHz, $CDCl_3$/acetone-d_6): δ = 185.8, 147.4, 147.3, 147.2, 147.1, 135.4, 135.1, 134.9, 134.8, 133.7, 132.9, 132.7, 132.5, 131.9, 131.8, 131.8, 131.7, 131.4, 130.7, 130.5, 130.4, 130.4, 129.9, 128.4, 120.6, 120.5, 120.3, 120.1, 119.9, 102.9, 66.5, 66.0, 35.5, 35.5, 35.3, 30.8, 30.5, 30.3, 30.0, 29.8, 29.6 ppm; FT-IR(KBr): v = 3431.7 (w), 3261.5 (w), 3000.0 (w), 2957.0 (m), 2918.7 (w), 2865.2 (w), 1638.7 (w), 1595.9 (s), 1485.9 (m), 1454.0 (m), 1387.9 (w), 1361.0 (s), 1335.5 (w), 1298.4 (m), 1261.2 (m), 1204.2 (w), 1088.9 (m), 1027.8 (m), 997.5 (w), 940.0 (w), 929.7 (w), 887.1 (w), 837.1 (w), 819.4 (w) cm^{-1}; MALDI-TOF-MS (dithranol): calc'd for $[C_{77}H_{94}N_4O_5Na]^+$ = 1177.71; found: $[C_{77}H_{94}N_4O_5Na]^+$ = 1177.03 ($[M + Na]^+$); UV/Vis (CH_2Cl_2): 345, 510 (λ_{max}) nm.

N-Alkylation of OxP-CH_2OH. OxP-CH_2OH exhibits lower reactivity and selectivity for N-alkylation compared to **OxP-CHO**. Alkylation of OxP-CH_2OH resulted tetra-N-alkylated **Bn_4OxP-CH_2OH** and two regioisomers of the dialkylated product i.e. N_{21},N_{23}-dialkylated (minor product) and N_{22},N_{24}-dikylated (major product) along with unreacted starting material. **OxP-CH_2OH** (180 mg, 0.16 mmol) was dissolved in acetone. 4-Bromobenzyl bromide (78 mg, 0.31 mmol) and sodium carbonate (660 mg, 6.23 mmol) were added and the resulting mixture was refluxed under N_2 atmosphere. The reaction was monitored continuously using t.l.c. A further aliquot of 4-bromobenzyl bromide (78 mg, 0.31 mmol) was added after ~2 h. Four further equivalents of 4-bromobenzyl bromide was added after 4 h and the reaction was continuously monitored for the following 6 h. Three product spots appeared in addition to that due to residual starting material. Solvent was removed under reduced pressure and the resulting solid was partitioned between dichloromethane (60 mL) and water (100 mL). The highly colored dichloromethane fraction was dried over anhydrous sodium sulfate then filtered and the solvents removed under reduced pressure. The resulting solid was chromatographed on silica gel using gradient elution (hexane/dichloromethane). Tetra-N-alkylated porphyrinogen **Bn_4OxP-CH_2OH** was obtained under elution at hexane:dichloromethane 1:1. The regioisomeric mixture of di-N-alkylated products was eluted at hexane:dichloromethane 3:7. The regioisomeric mixture of di-N-alkylated products was separated using preparative thin layer chromatography (PTLC). The final yields of products obtained after separation were N_{21},N_{23}-**Bn_2OxP-CH_2OH** (minor isomer, 7 mg, 3 %), N_{22},N_{24}-**Bn_2OxP-CH_2OH** (major isomer, 50 mg, 21.5 %), and **Bn_4OxP-CH_2OH** (40 mg, 14 %).

N_{21},N_{23}-Bis(4-bromobenzyl)-2-hydroxymethyl-5,10,15,20-tetrakis(3,5-di-*tert*-butyl-4-oxo-cyclohexa-2,5-dienylidene)porphyrinogen (Bn_2OxP-CH_2OH Minor)

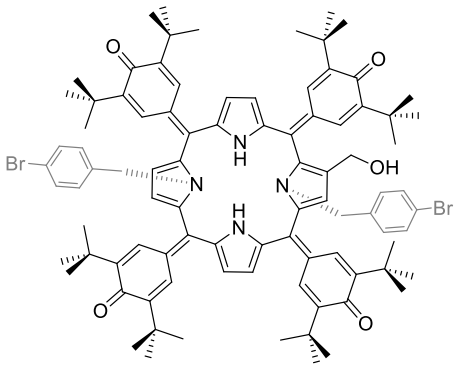

^{1}H NMR (300 MHz, $CDCl_3$): δ = 9.33 (s, 1H), 9.19 (s, 1H), 7.51-7.69 (m, 4H), 7.27-7.29 (m, 1H), 7.24 (d, J = 2.4 Hz, 1H), 6.87-7.19 (m, 8H), 6.51-6.79 (m, 9H), 4.56 (d, J = 12.1 Hz, 1H), 4.31-4.44 (m, 4H), 4.10 (d, J = 12.1 Hz, 1H), 1.17-1.38 (m, 72H) ppm; FT-IR(KBr): ν = 3431.9 (w), 3237.8 (w), 2996.9 (w), 2955.4 (m), 2923.6 (w), 2860.3 (w), 1727.3 (w), 1596.7 (s), 1533.1 (w), 1489.0 (m), 1458.3 (m), 1454.1 (m), 1405.2 (w), 1387.5 (w), 1360.9 (m), 1335.3 (w), 1312.8 (w), 1256.8 (w), 1087.1 (m), 1072.6 (m), 1028.3 (w), 1012.8 (w), 983.0 (w), 955.7 (w), 929.6 (w) cm^{-1}; MALDI-TOF-MS (dithranol): calc'd for $[C_{91}H_{105}Br_2N_4O_5Na]^+$ = 1514.63; found: $[C_{91}H_{105}Br_2N_4O_5Na]^+$ = 1514.51 ($[M + Na + H]^+$); UV/Vis (CH_2Cl_2): 332, 504 (λ_{max}) nm.

N_{22},N_{24}-Bis(4-bromobenzyl)-2-hydroxymethyl-5,10,15,20-tetrakis(3,5-di-*tert*-butyl-4-oxo-cyclohexa-2,5-dienylidene)porphyrinogen (Bn_2OxP-CH_2OH Major).

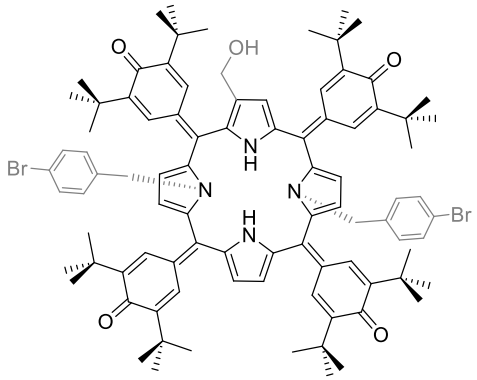

^{1}H NMR (300 MHz, $CDCl_3$): δ = 10.52 (s, 1H), 9.73 (s, 1H), 7.60-7.64 (m, 3H), 7.53 (s, 1H), 6.84-7.02 (m, 9H), 6.54-6.73 (m, 10H), 4.31-4.51 (m, 4H), 4.17 (d, J = 9.2 Hz, 1H), 3.90 (d, J = 9.2 Hz, 1H), 1.19-1.36 (m, 72H) ppm; ^{13}C NMR (76 MHz, $CDCl_3$): δ = 186.2, 186.1, 186.0, 185.9, 148.8, 148.6, 148.5, 148.3, 148.2, 147.5, 147.5, 147.5, 137.0, 136.5, 135.8, 135.7, 135.6, 135.5, 135.5, 135.3, 135.0, 133.9, 133.2, 132.5, 132.1, 132.1, 131.9, 131.9, 131.7, 131.5, 131.3, 131.3, 130.9, 130.9, 130.8, 130.5, 130.5, 129.2, 129.0, 128.8, 127.8, 122.4, 122.3, 120.8, 120.4, 119.8, 119.6, 119.3, 119.1, 118.9, 66.8, 35.8, 35.8, 35.7, 35.7, 35.4, 35.4, 35.4, 29.7, 29.6, 29.6, 29.6, 15.3 ppm; FT-IR(KBr): ν = 3421.9 (w), 2999.6 (w), 2956.7 (m), 2865.34 (w), 1733.2 (w), 1597.4 (s), 1546.9 (w), 1488.38 (m), 1455.0 (m), 1388.3 (w), 1361.2 (s), 1316.5 (w), 1256.8 (w), 1087.1 (m), 1072.5 (m), 1027.5 (m), 1012.6 (w), 982.2 (w), 949.1 (m), 929.5 (w), 915.6 (w) cm^{-1}; MALDI-TOF-MS (dithranol): calc'd for $[C_{91}H_{107}Br_2N_4O_5Na]^+$ = 1516.65; found: $[C_{91}H_{107}Br_2N_4O_5Na]^+$ = 1516.77 ($[M + Na + 3H]^+$); UV/Vis (CH_2Cl_2): 332, 507 (λ_{max}) nm.

N_{21},N_{22},N_{23},N_{24}-tetrakis(4-bromobenzyl)-2-hydroxymethyl-5,10,15,20-tetrakis(3,5-di-*tert*-butyl-4-oxo-cyclohexa -2,5-dienylidene)porphyrinogen (Bn_4OxP-CH_2OH).

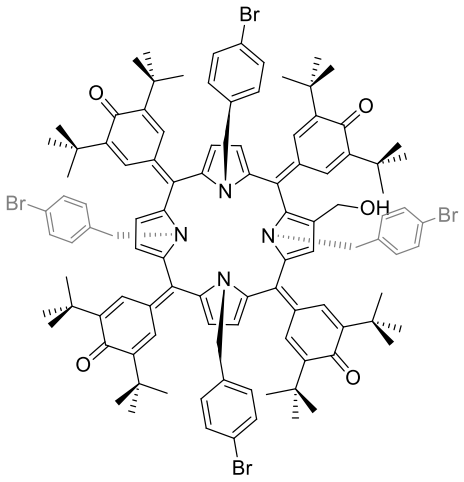

^{1}H NMR (300 MHz, $CDCl_3$): δ = 7.44-7.50 (m, 1H), 7.40 (d, J = 2.2 Hz, 1H), 7.27-7.33 (m, 11H), 7.10-7.22 (m, 4H), 6.51-6.76 (m, 14H), 4.73-4.78 (m, 1H), 4.36-4.53 (m, 6H), 4.24-4.33 (m, 1H), 4.14 (d, J = 11.5 Hz, 1H), 3.81 (d, J = 11.5 Hz, 1H), 1.21-1.32 (m, 72H) ppm; ^{13}C NMR (76 MHz, $CDCl_3$): δ = 185.9, 185.9, 149.2, 148.8, 148.6, 138.7, 138.3, 138.3, 138.1, 137.1, 136.9, 136.9, 136.8, 136.7, 136.6, 136.5, 136.4, 136.4, 136.3, 134.9, 134.6, 134.5, 134.3, 134.3, 134.2, 134.1, 132.1, 132.0, 131.9, 131.8, 131.0, 130.9, 130.7, 130.6, 130.5, 129.9, 129.9, 129.7, 129.7, 129.6, 128.5, 128.4, 128.2, 128.2, 128.1, 128.1, 127.9, 127.8, 127.5, 127.5, 122.3, 122.1, 122.0, 121.0, 120.8, 120.7, 66.6, 65.5, 48.2, 48.1, 48.0, 35.7, 35.6, 29.5, 29.4 ppm; FT-IR(KBr): ν = 2956.5 (s), 2921.2 (m), 2864.7 (m), 1598.1 (s), 1525.5 (w), 1489.0 (m), 1455.0 (m), 1405.4 (w), 1388.1 (w), 1360.9 (m), 1312.9 (w), 1256.5 (w), 1170.6 (w), 1087.2 (m), 1072.7 (m), 1011.7 (w), 960.2 (w), 865.2 (w) cm^{-1}; MALDI-TOF-MS (dithranol): calc'd for $[C_{105}H_{115}Br_4N_4O_5Na]^+$ = 1850.54; found: $[C_{105}H_{115}Br_4N_4O_5Na]^+$ = 1850.14 ([M + H + Na]$^+$); UV/Vis (CH_2Cl_2): 330, 501 (λ_{max}) nm.

N_{21},N_{23}-Bis(4-bromobenzyl)-2-(5,6-dicyano-1*H*-imidazo[4,5-*b*]pyrazin-2-yl)-5,10,15,20-tetrakis(3,5-di-*tert*-butyl-4-oxo-cyclohexa-2,5-dienylidene)porphyrinogen (1).

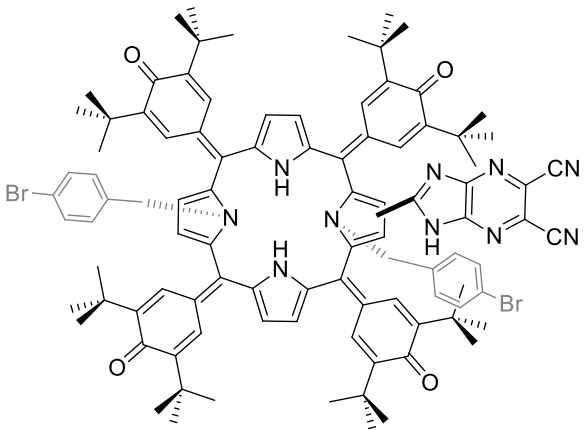

A mixture of **Bn_2OxP-CHO** (200 mg, 0.13 mmol) and 5,6-diamino-2,3-dicyanopyrazine (86 mg, 0.54 mmol) in dimethylformamide (4 mL) was refluxed for 60 h. After completion of the reaction, the mixture was cooled to room temperature and solvent was removed under reduced pressure. The residue was subjected to column chromatography on SiO_2 eluting with 0.5% acetone in dichloromethane. Product containing fractions were combined and the solvents removed under reduced pressure. The resulting residue was further purified using gel permeation chromatography (BioBeads SX-1) eluting with dichloromethane. Yield: 100 mg (46 %).

1

^{1}H NMR (300 MHz, $CDCl_3$): δ 9.46 (s, 1H), 9.26 (s, 1H), 7.77 (d, J = 2.2 Hz, 1H), 7.66 (d, J = 2.2 Hz, 1H), 7.60 (d, J = 2.2 Hz, 1H), 7.56 (d, J = 2.2 Hz, 1H), 7.43 (s, 1H), 7.29-7.32 (m, 2H), 7.24 (s, 1H), 6.80-7.11 (m, 10H), 6.48-6.62 (m, 5H), 4.45-4.66 (m, 2H), 4.26-4.38 (m, 2H), 1.21-1.40 (m, 72H) ppm; ^{13}C NMR (76 MHz, $CDCl_3$/acetone-d_6): δ = 186.2, 186.1, 185.2, 159.5, 150.8, 150.8, 149.6, 149.5, 149.3, 149.3, 149.0, 149.0, 148.7, 148.7, 148.0, 142.0, 142.0, 137.5, 136.5, 136.0, 135.8, 134.6, 134.4, 134.1, 133.4, 133.0, 132.9, 132.3, 132.0, 131.6, 131.5, 130.9, 130.5, 130.3, 130.1, 130.0, 129.5, 129.4, 129.3, 128.7, 128.7, 127.0, 125.3, 123.2, 122.4, 120.5, 120.3, 120.0, 119.8, 118.8, 118.8, 113.9, 49.3, 48.6, 36.0, 35.9, 35.8, 35.8, 35.7, 35.5, 35.2, 35.2, 30.6, 30.4, 30.1, 30.1, 29.9, 29.8, 29.6 ppm; FTIR (KBr): ν = 3314.5 (w), 2999.3 (w), 2957.2 (s), 2865.9 (w), 2237.0 (w), 1600.0 (s), 1544.8 (w), 1489.0 (m), 1455.1 (m), 1409.6 (w), 1388.6 (w), 1361.9 (s), 1334.0 (w), 1312.8 (m), 1257.7 (m), 1178.2 (w), 1087.1 (m), 1072.7 (m), 1028.2 (m), 1012.9 (w), 948.2 (m) cm^{-1}; MALDI-TOF-MS (dithranol): calc'd for $[C_{97}H_{102}N_{10}O_4Br_2]^+$ = 1628.64; found: $[C_{97}H_{102}N_{10}O_4Br_2]^+$ = 1628.41 ($[M]^+$); UV/Vis (CH_2Cl_2): 265, 334, 503 (λ_{max}) nm.

N_{21},N_{22},N_{23},N_{24}-tetrakis(4-bromobenzyl)-2-(5,6-dicyano-1*H*-imidazo[4,5-*b*]pyrazin-2-yl)-5,10,15,20-tetrakis(3,5-di-*tert*-butyl-4-oxo-cyclohexa-2,5-dienylidene)porphyrinogen (2).

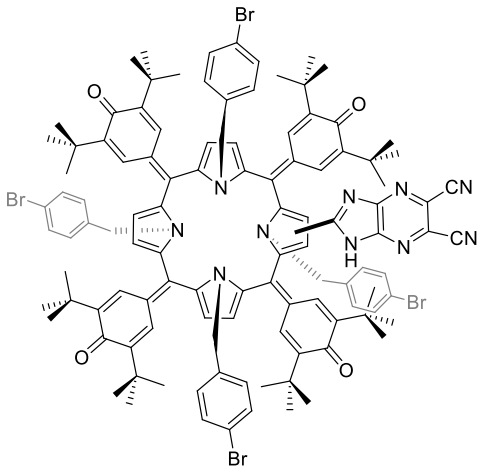

2 was prepared and purified using the same procedure as for **1** using **Bn_4OxP-CHO** (200 mg, 0.11 mmol) and 5,6-diamino-2,3-dicyanopyrazine (70 mg, 0.44 mmol). Yield: 105 mg (49 %).

^{1}H NMR in $CDCl_3$ (MHz): δ 8.00 (s, 1H), 7.65 (s, 1H), 7.30-7.38 (m, 12H), 7.06-7.20 (m, 4H), 6.85-6.92 (m, 3H), 6.63-6.74 (m, 7H), 6.51-6.56 (m, 3H), 6.15 (d, J = 8.4 Hz, 1H), 4.10-4.86 (m, 8H), 1.24-1.41 (m, 72H) ppm; ^{13}C NMR ($CDCl_3$, 75 MHz): δ 186.1, 185.9, 151.4, 149.3, 149.0, 148.9, 138.7, 137.8, 137.6, 137.6, 136.1, 136.0, 135.3, 132.7, 132.4, 132.3, 132.3, 132.1, 131.9, 130.7, 129.8, 129.7, 129.0, 128.7, 128.4, 128.2, 128.1, 127.7, 126.4, 126.2, 126.1, 123.3, 123.0, 122.9, 122.8, 122.5, 121.2, 120.5, 120.3, 117.0, 116.8, 113.9, 113.8, 48.8, 48.6, 48.1, 48.0, 36.2, 36.1, 35.7, 35.5, 29.9, 29.7, 29.4, 29.1 (ppm); FT-IR(KBr): ν = 2956.9 (s), 2923.9 (m), 2865.5 (w), 2235.6 (w), 1725.1 (m), 1604.7 (s), 1525.4 (w), 1489.0 (m), 1455.0 (m), 1408.5 (w), 1388.4 (w), 1361.3 (M), 1320.5 (m), 1256.4 (w), 1087.7 (m), 1072.6 (m), 1011.9 (m) cm^{-1}; MALDI-TOF-MS (dithranol): calc'd for $[C_{111}H_{114}N_{10}O_4Br_4]^+$ = 1966.57; found: $[C_{111}H_{114}N_{10}O_4Br_4]^+$ = 1966.34 ($[M + H]$)$^+$; UV/Vis (CH_2Cl_2): 270, 335, 497 (λ_{max}) nm.

Compounds 3(a-c)

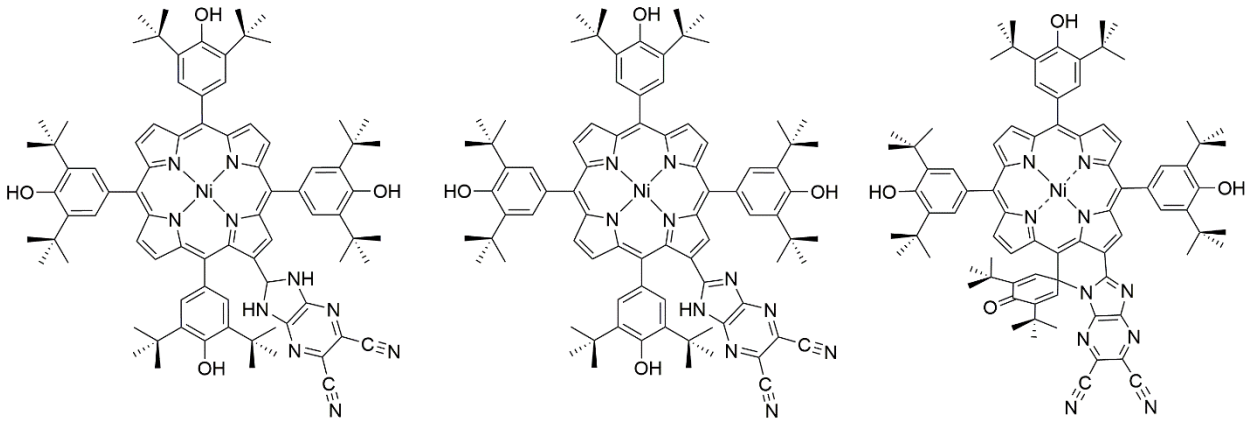

A mixture of [T(DtBHP)PNi]-CHO[S9] (300 mg, 0.25 mmol) and 5,6-diamino-2,3-dicyanopyrazine (158 mg, 0.98 mmol) in dimethylformamide (8 mL) was refluxed for 60 h. After completion of the reaction, the mixture was cooled to room temperature and solvent was removed under reduced pressure. The residue was purified by column chromatography (SiO_2), elution with hexane/dichloromethane (1:1) gave **(a)** as a greenish solid (Yield: 160 mg, 48%) followed by elution of **(b)** as a dark green solid (Yield: 70 mg, 21%) with hexane/dichloromethane (4:6, v/v), further elution with dichloromethane gave **(c)** as a reddish solid (Yield: 150 mg, 45%).

(3a): ^{1}H NMR in $CDCl_3$ (MHz): δ 8.95 (s, 1H), 8.70-8.80 (m, 6H), 7.73-7.77 (m, 8H), 6.82 (s, 1H), 5.92 (s, 2H), 5.70 (s, 1H), 5.48-5.53 (m, 3H), 1.50-1.56 (m, 72H); MALDI-TOF-MS (dithranol): calc'd for $[C_{83}H_{95}N_{10}NiO_4]^+$ = 1353.68; found: $[C_{83}H_{93}N_{10}NiO_4]^+$ = 1353.65 ($[M + H]$)$^+$; UV/Vis (CH_2Cl_2): 428 (λ_{max}), 538 nm.

(3b): ^{1}H NMR in $CDCl_3$ (MHz): δ 9.63 (s, 1H), 8.72-8.81 (m, 6H), 8.55 (d, J = 4.8 Hz, 1H), 7.88 (s, 2H), 7.75-7.79 (m, 6H), 5.47-5.53 (m, 4H), 1.54-1.58 (m, 55H), 1.36 (s, 17H); MALDI-TOF-MS (dithranol): calc'd for $[C_{83}H_{93}N_{10}NiO_4]^+$ = 1351.67; found: $[C_{83}H_{93}N_{10}NiO_4]^+$ = 1351.53 ($[M + H]$)$^+$; UV/Vis (CH_2Cl_2): 410 (λ_{max}), 462 (λ_{max}), 556, 607 nm.

(3c): ^{1}H NMR in $CDCl_3$ (MHz): δ 9.74 (s, 1H), 9.33 (d, J = 5.1 Hz, 1H), 8.94 (d, J = 5.1 Hz, 1H), 8.75-8.83 (m, 4H), 7.82 (s, 2H), 7.74-7.77 (m, 4H), 7.08 (s, 2H), 5.61 (s, 1H), 5.53 (s, 1H), 5.52 (s, 1H), 1.54-1.61 (m, 72H); MALDI-TOF-MS (dithranol): calc'd for $[C_{83}H_{93}N_{10}NiO_4]^+$ = 1351.67; found: $[C_{83}H_{93}N_{10}NiO_4]^+$ = 1351.63 ($[M + 3H]$)$^+$; UV/Vis (CH_2Cl_2): 403, 462 (λ_{max}), 616 nm.

References

S1. E. R. Henry and J. Hofrichter, in *Methods in Enzymology*, Academic Press, 1992, vol. 210, pp. 129–192.

S2. E R. Malinowski, Factor Analysis in Chemistry. United States of America, New York: Wiley-Interscience, 2002, pp. 1–432.

S3. V. Březina, S. Ishihara, J. Lang, L. Hanyková, K. Ariga, J. P. Hill, J. Labuta, *ChemistryOpen*, 2018, **7**, 323.

S4. J. Hanuš, K. Chmelová, J. Štěpánek, P.-Y. Turpin, J. Bok, I. Rosenberg, Z. Točík, *J. Raman Spectrosc.*, 1999, **30**, 667.

S5. L. Zimányi *J. Phys. Chem. B*, 2004, **108**, 4199.

S6. L. Zimányi, Á. Kulcsár, J. K. Lanyi, D. F. Sears, J. Saltiel, *Proc. Nat. Acad. Sci. USA*, 1999, **96**, 4408.

S7. S. Alunni, A. Pero and G. Reichenbach, *J. Chem. Soc., Perkin Trans. 2*, 1998, 1747.

S8. J. P. Hill, I. J. Hewitt, C. E. Anson, A. K. Powell, A. L. McCarthy, P. A. Karr, M. E. Zandler and F. D'Souza, *J. Org. Chem.*, 2004, **69**, 5861.

S9. M. K. Chahal and M.Sankar, *Dalton Trans.*, 2016, **45**, 16404.

Appendix: NMR and Mass Spectra of the Compounds.

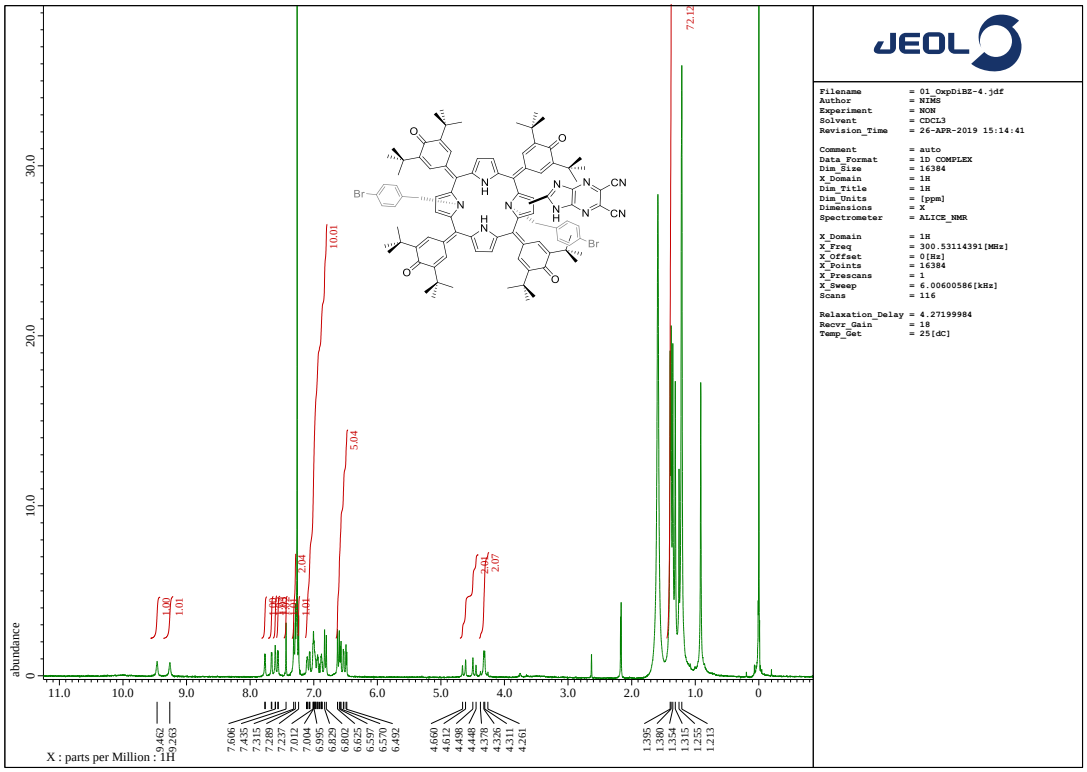

^{1}H NMR spectrum of **1** in $CDCl_3$.

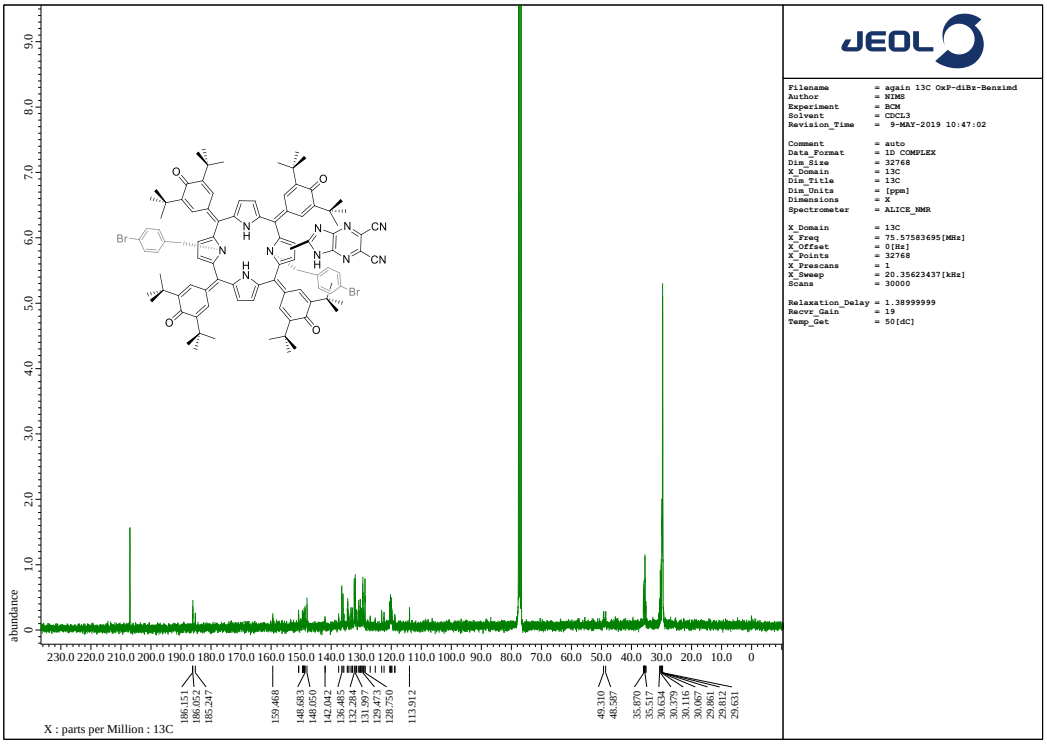

^{13}C NMR spectrum of **1** in $CDCl_3$/acetone-d_6.

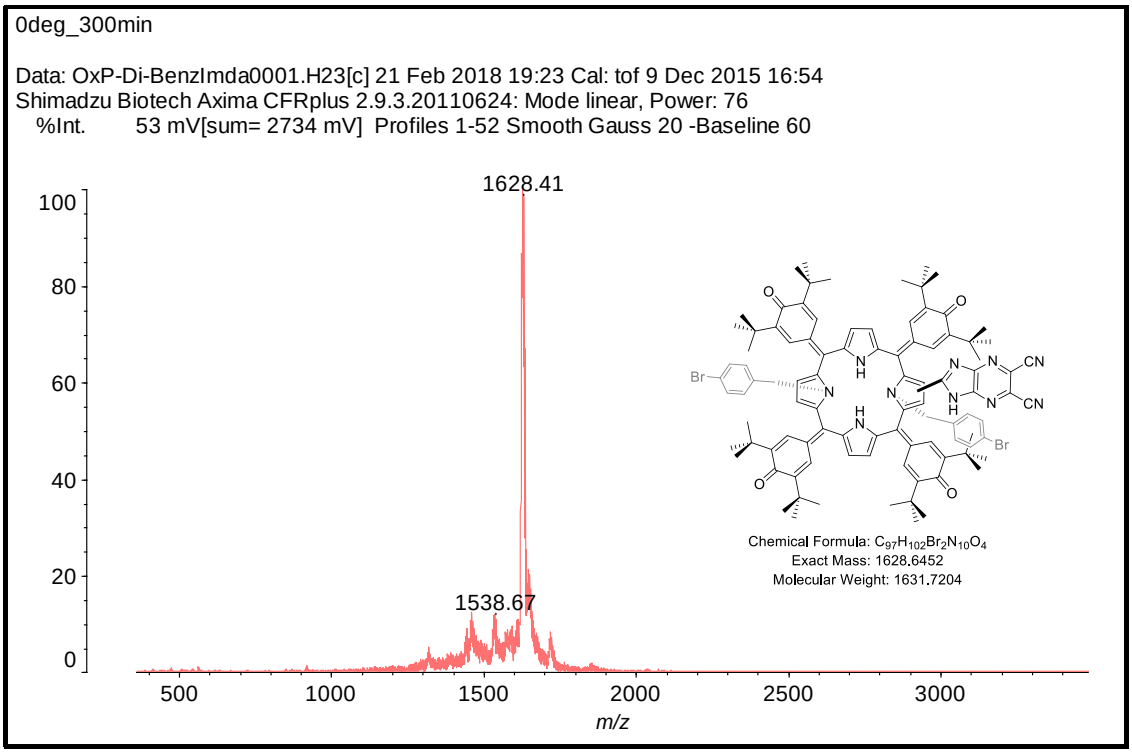

MALDI-TOF-MS mass spectrum of **1**.

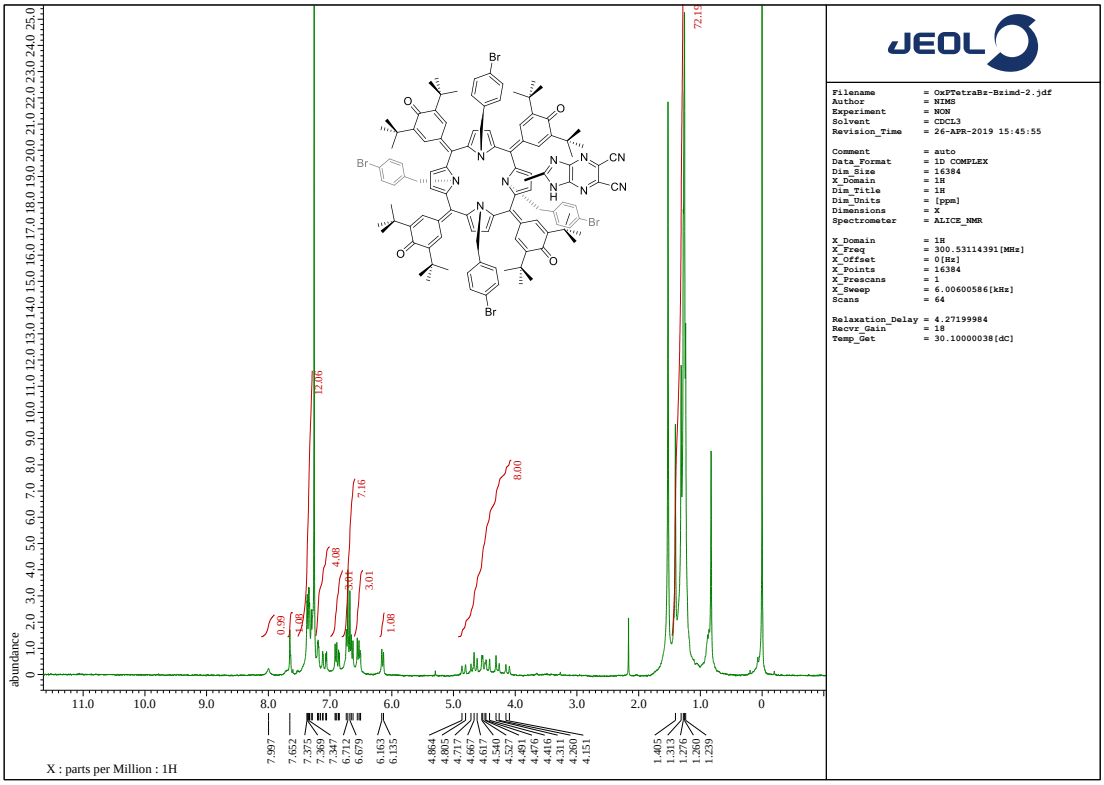

^{1}H NMR spectrum of **2** in $CDCl_3$.

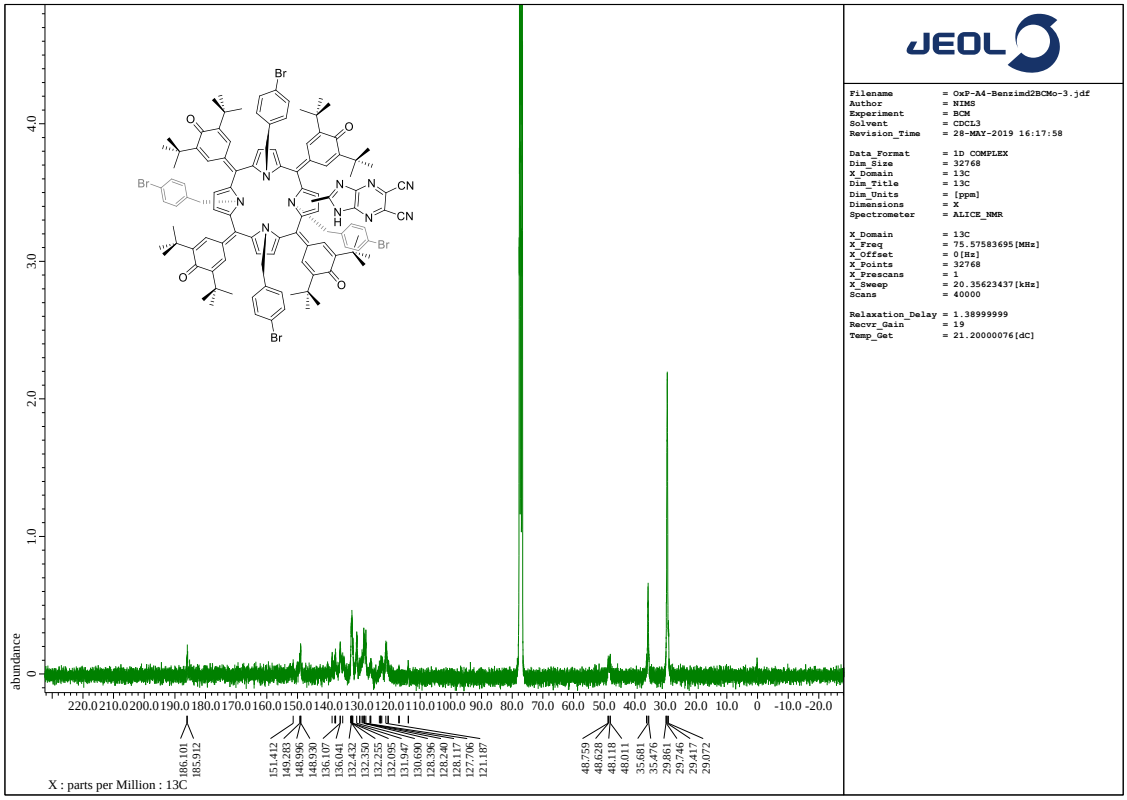

^{13}C NMR spectrum of **2** in $CDCl_3$.

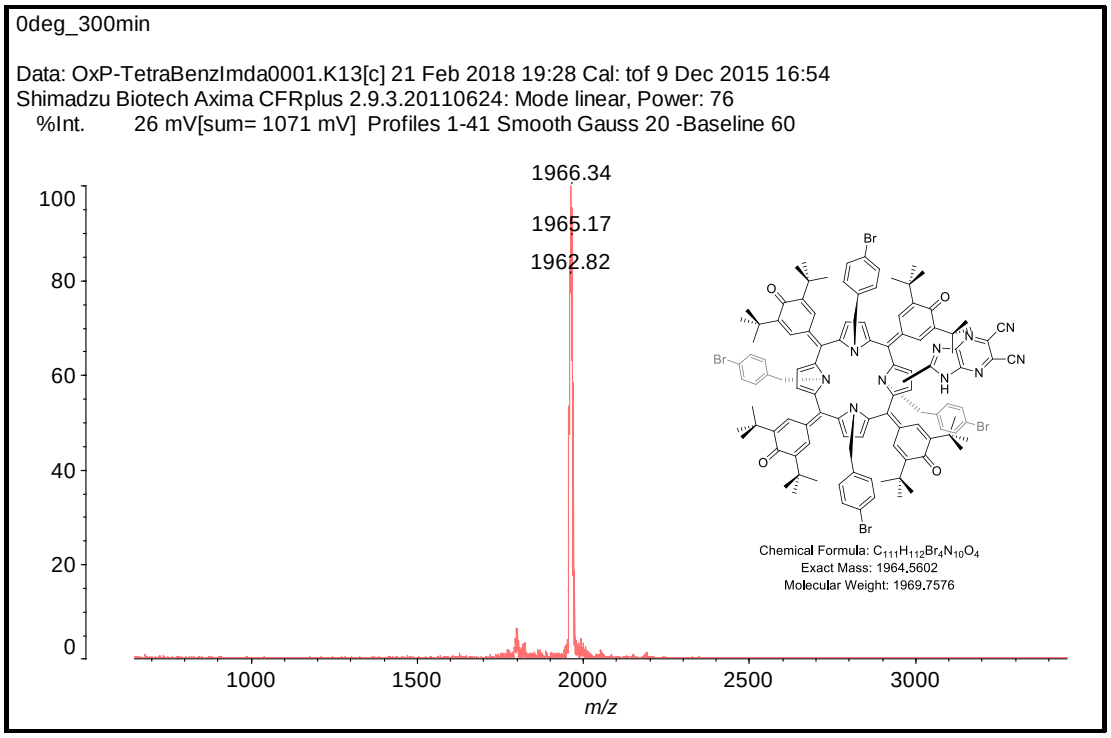

MALDI-TOF-MS mass spectrum of **2**.

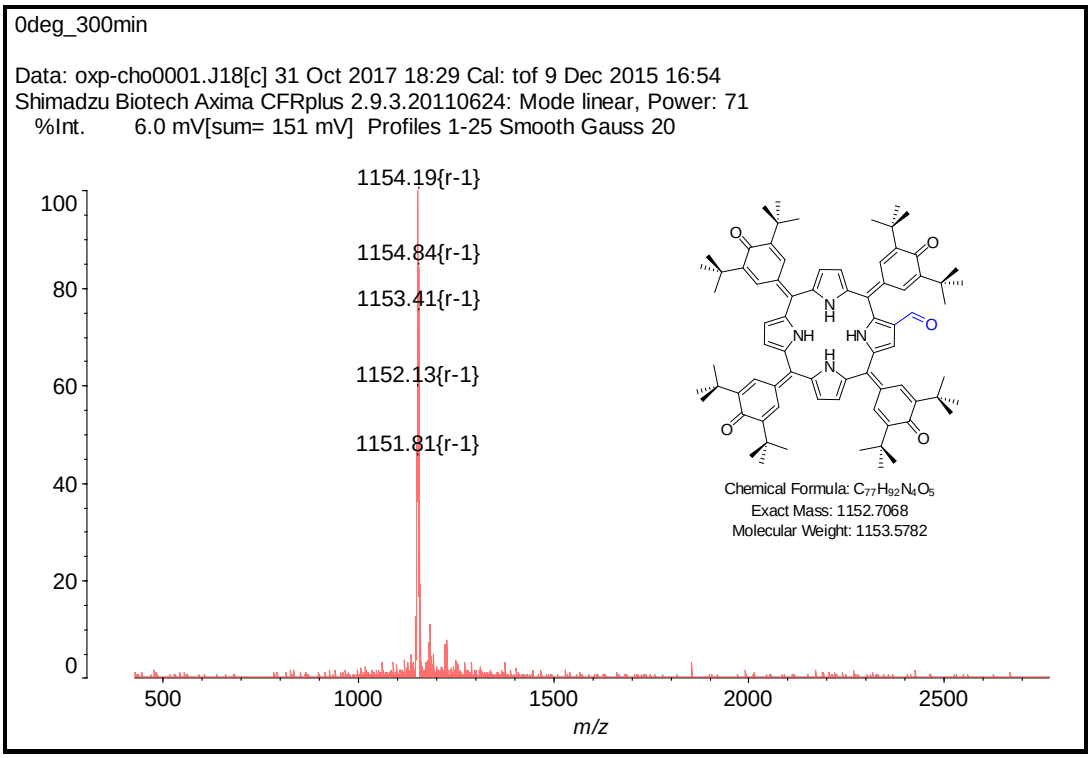

MALDI-TOF-MS mass spectrum of **OxP-CHO**.

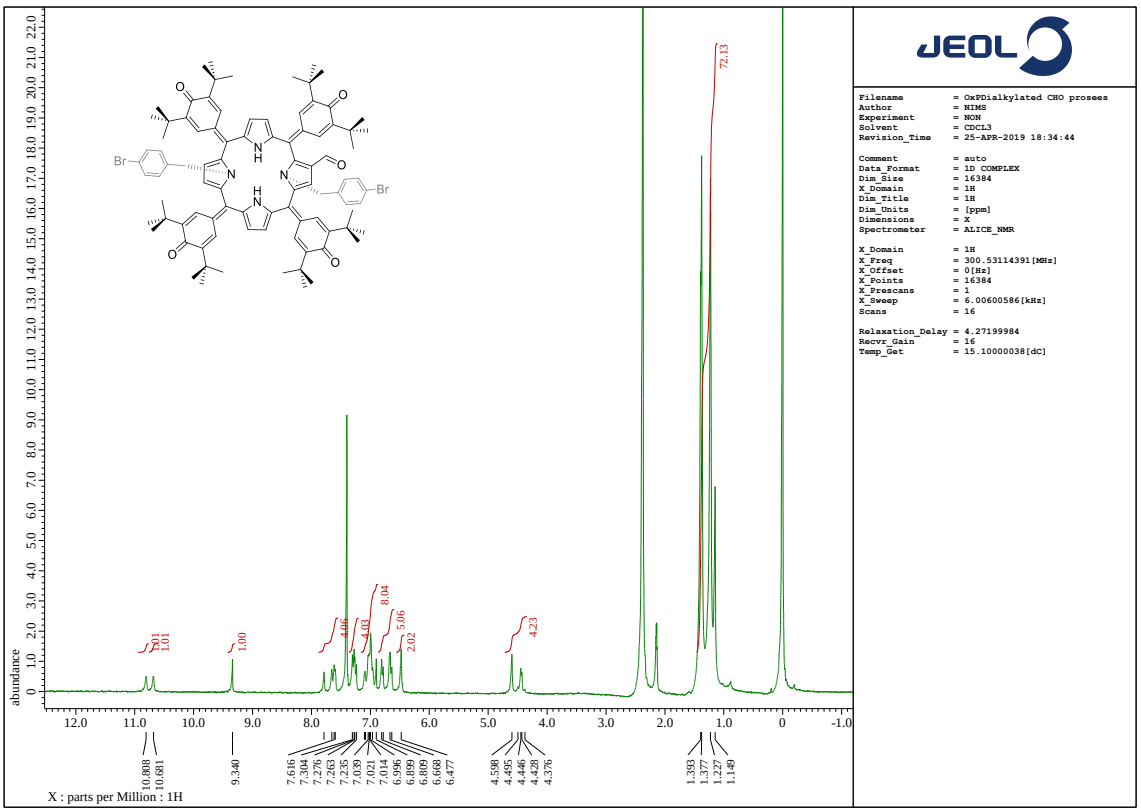

^{1}H NMR spectrum of **Bn$_2$OxP-CHO** in CDCl$_3$/acetone-*d*$_6$.

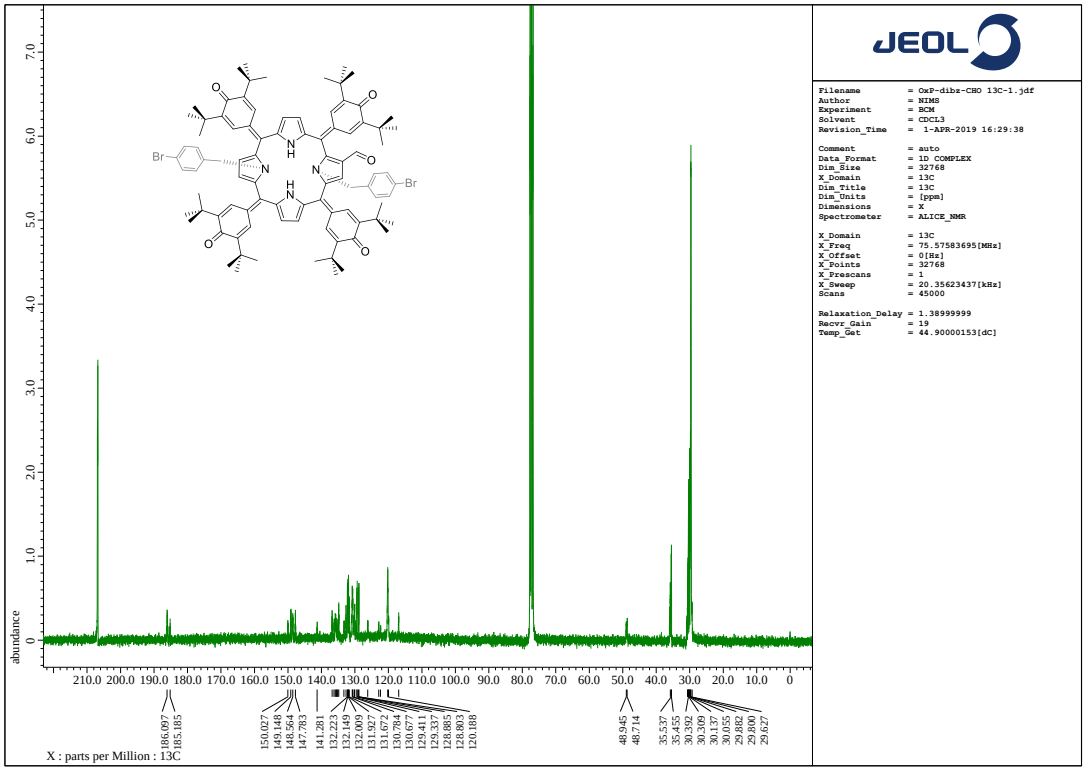

^{13}C NMR spectrum of **Bn$_2$OxP-CHO** in CDCl$_3$/acetone-*d*$_6$.

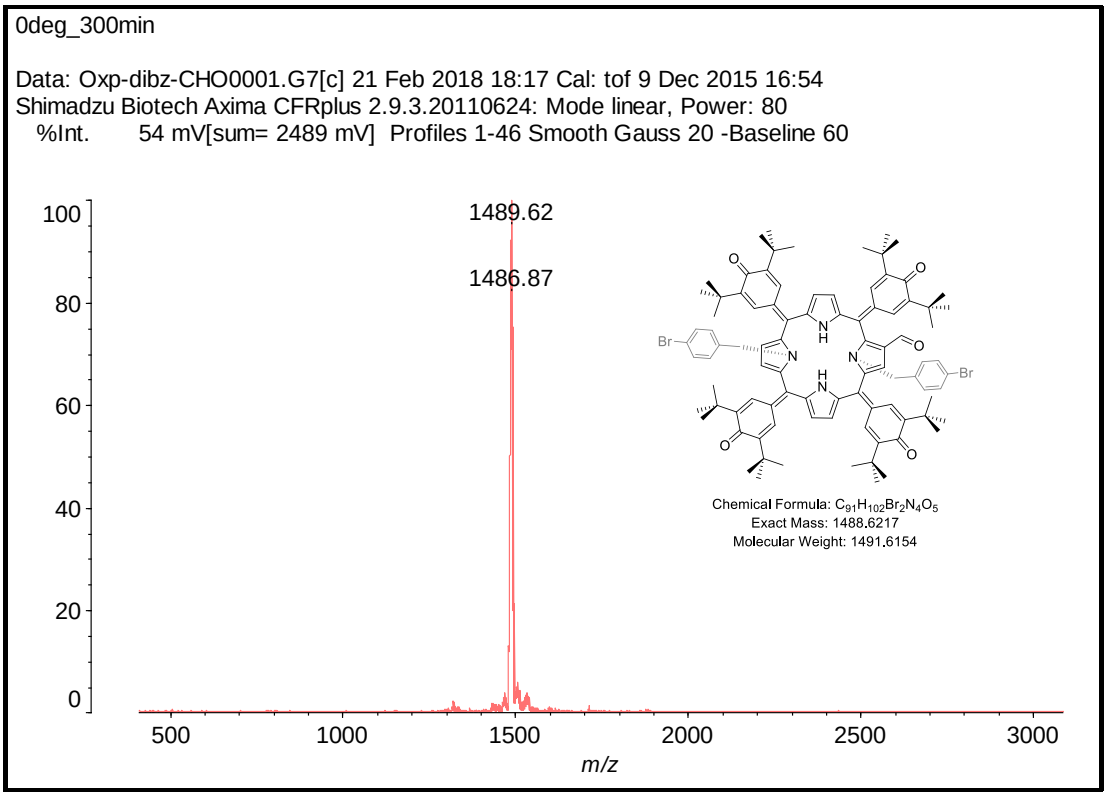

MALDI-TOF-MS mass spectrum of **Bn_2OxP-CHO**.

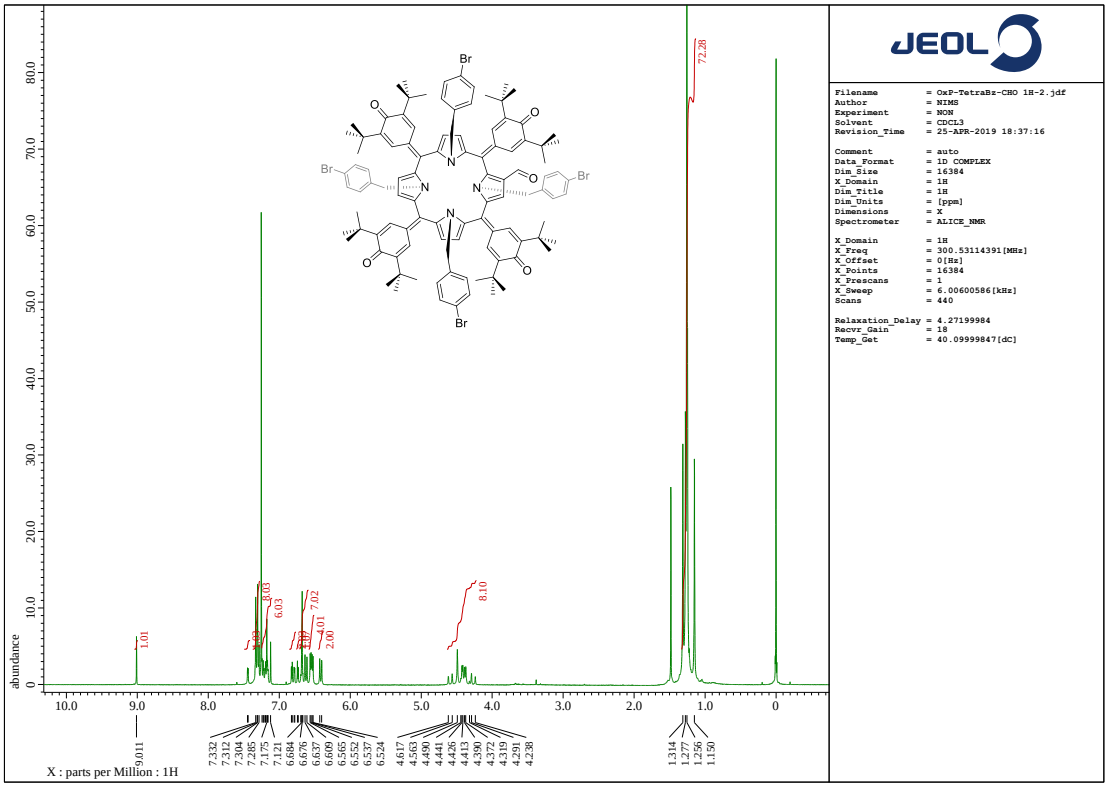

^{1}H NMR spectrum of **Bn$_4$OxP-CHO** in CDCl$_3$.

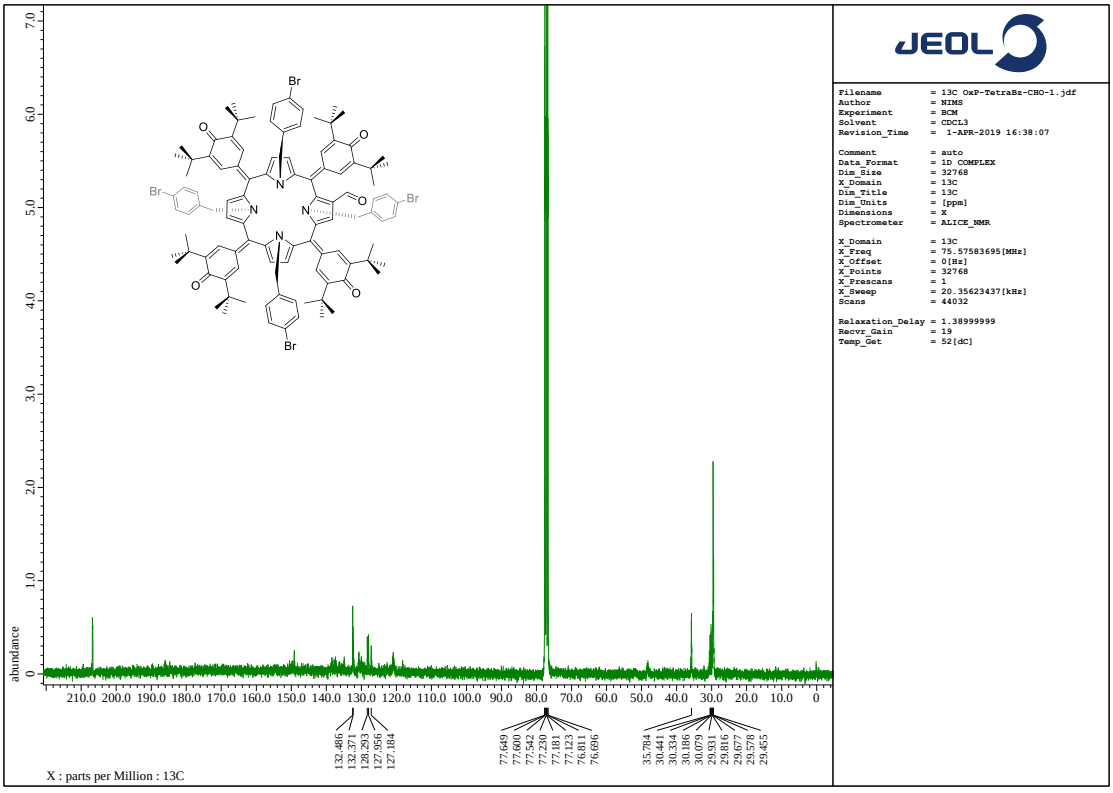

^{13}C NMR spectrum of **Bn$_4$OxP-CHO** in CDCl$_3$/acetone-*d$_6$*.

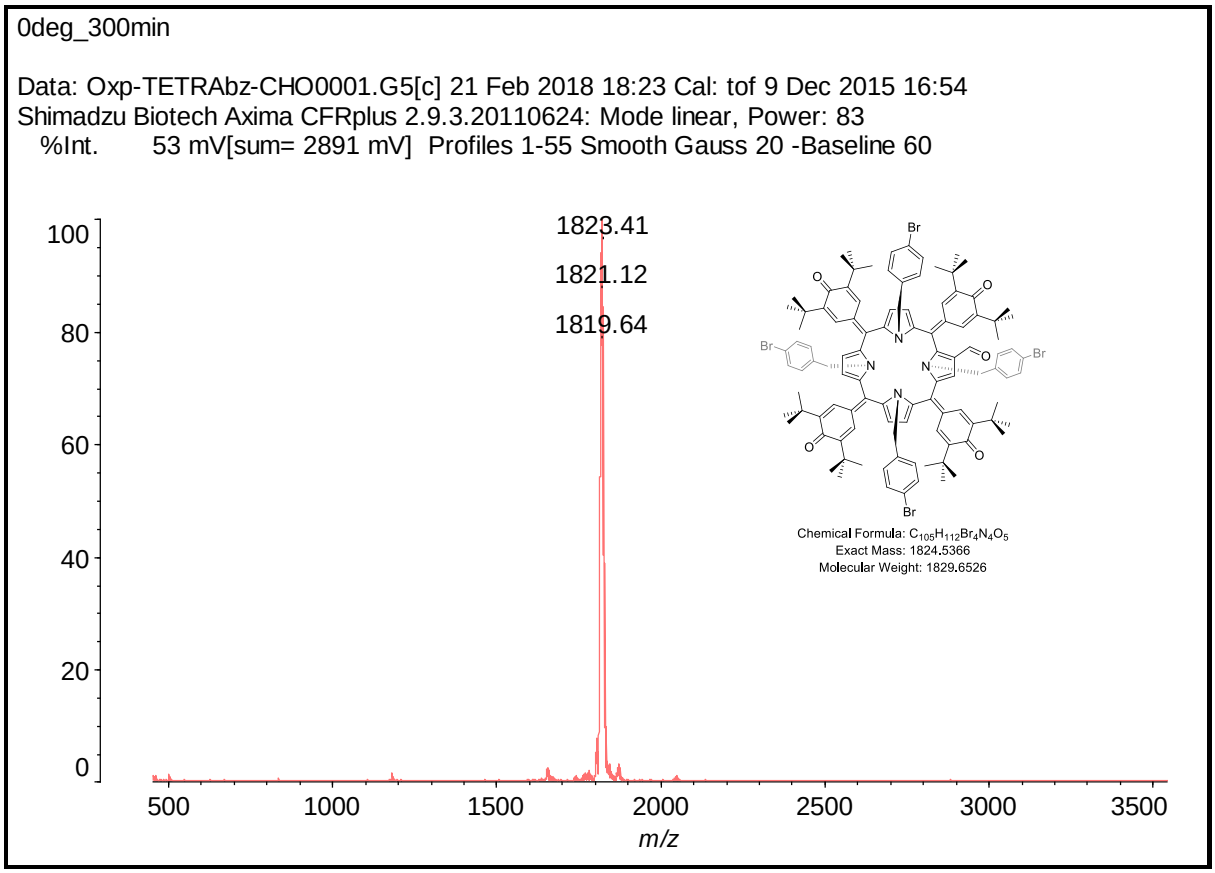

MALDI-TOF-MS mass spectrum of **Bn_4OxP-CHO**.

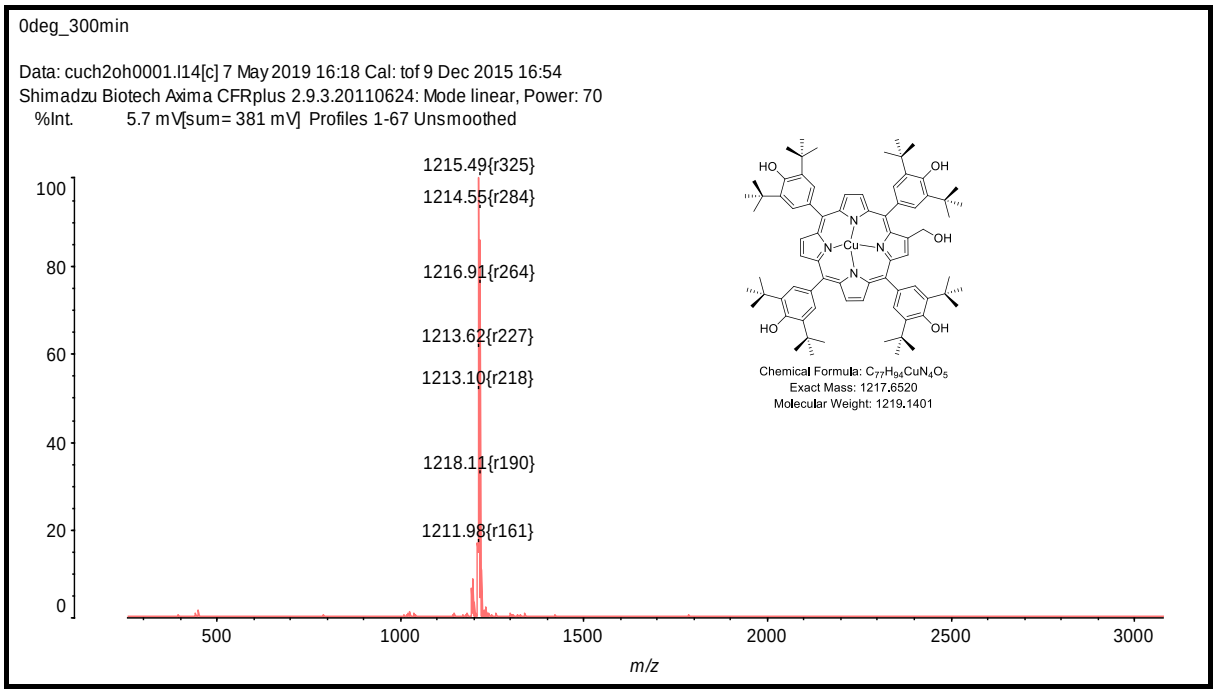

MALDI-TOF-MS mass spectrum of **[T(DtBHP)PCu]-CH_2OH**.

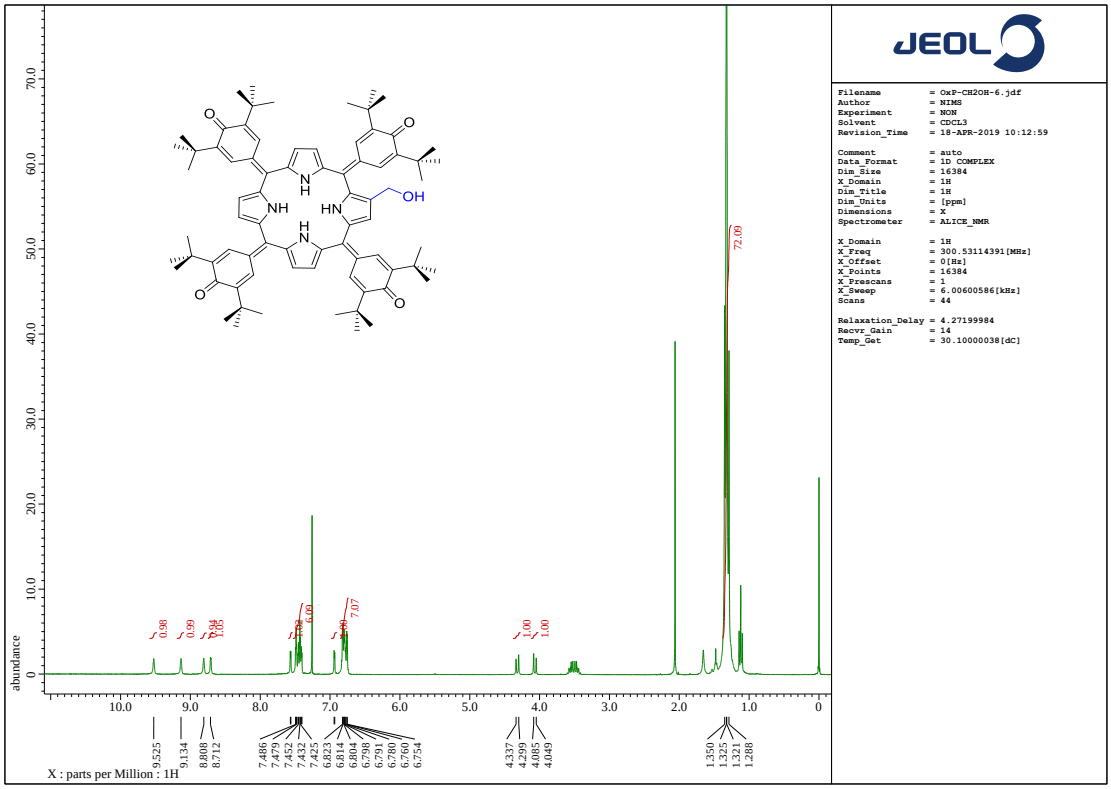

^{1}H NMR spectrum of **OxP-CH$_2$OH** in CDCl$_3$.

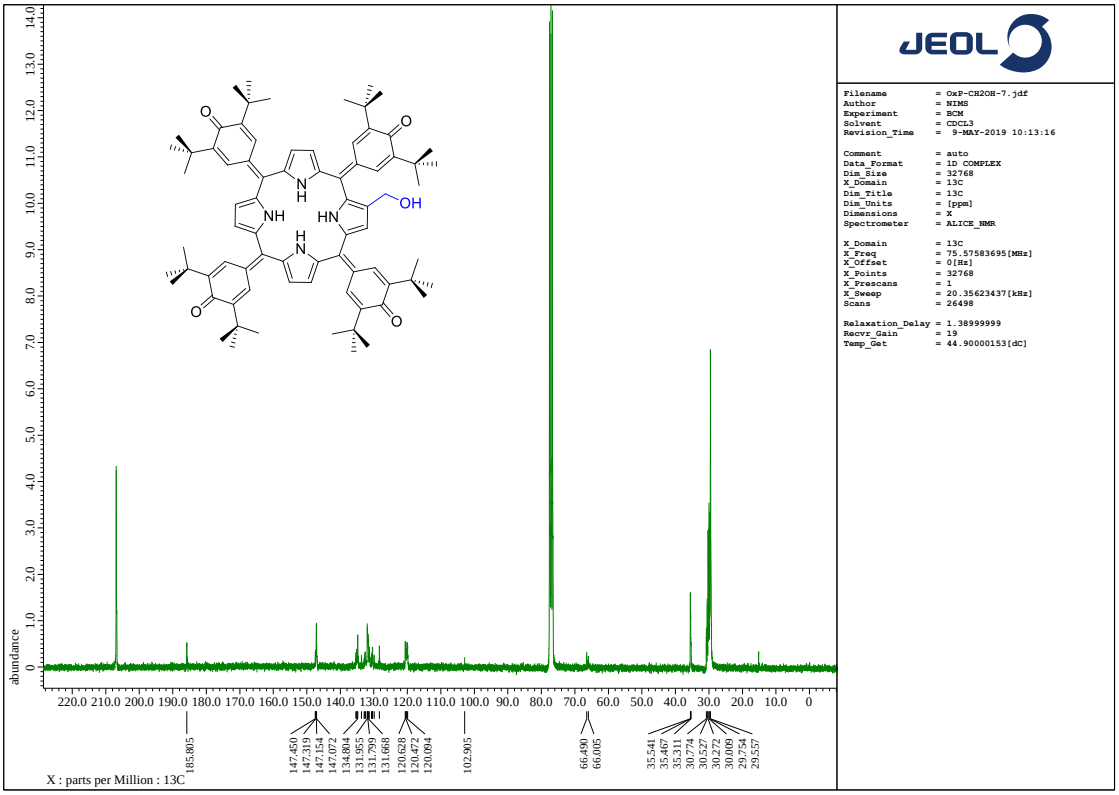

^{13}C NMR spectrum of **OxP-CH$_2$OH** in CDCl$_3$/acetone-*d$_6$*.

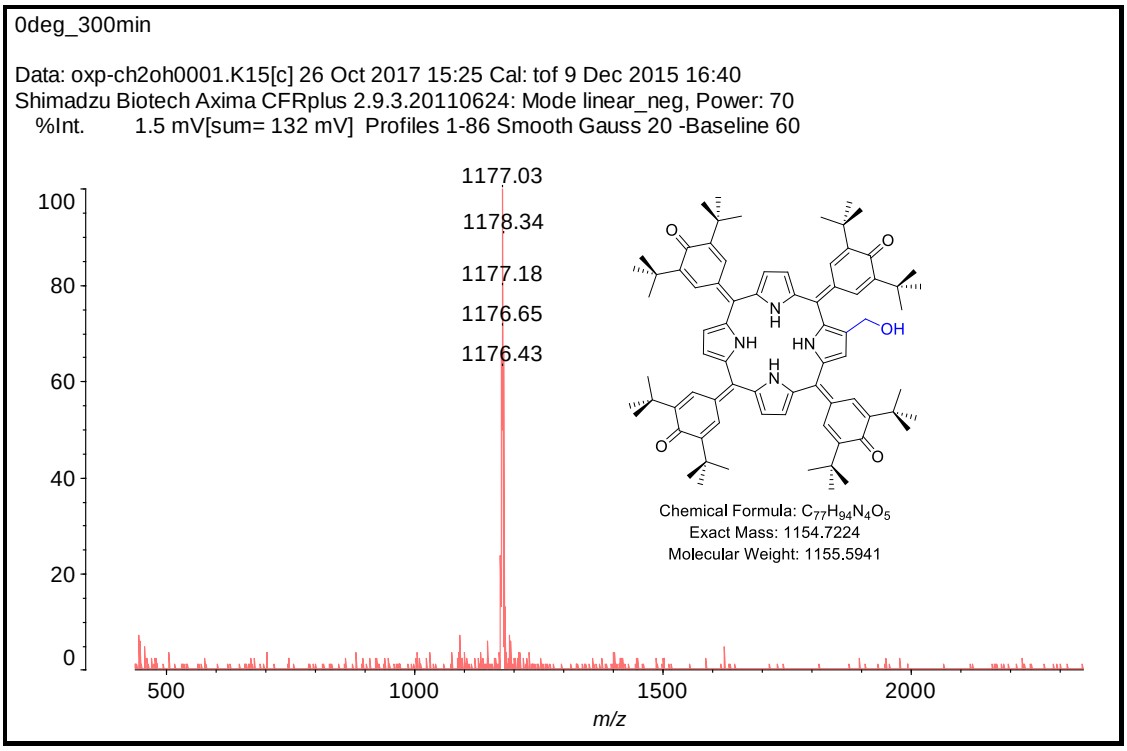

MALDI-TOF-MS mass spectrum of **OxP-CH$_2$OH**.

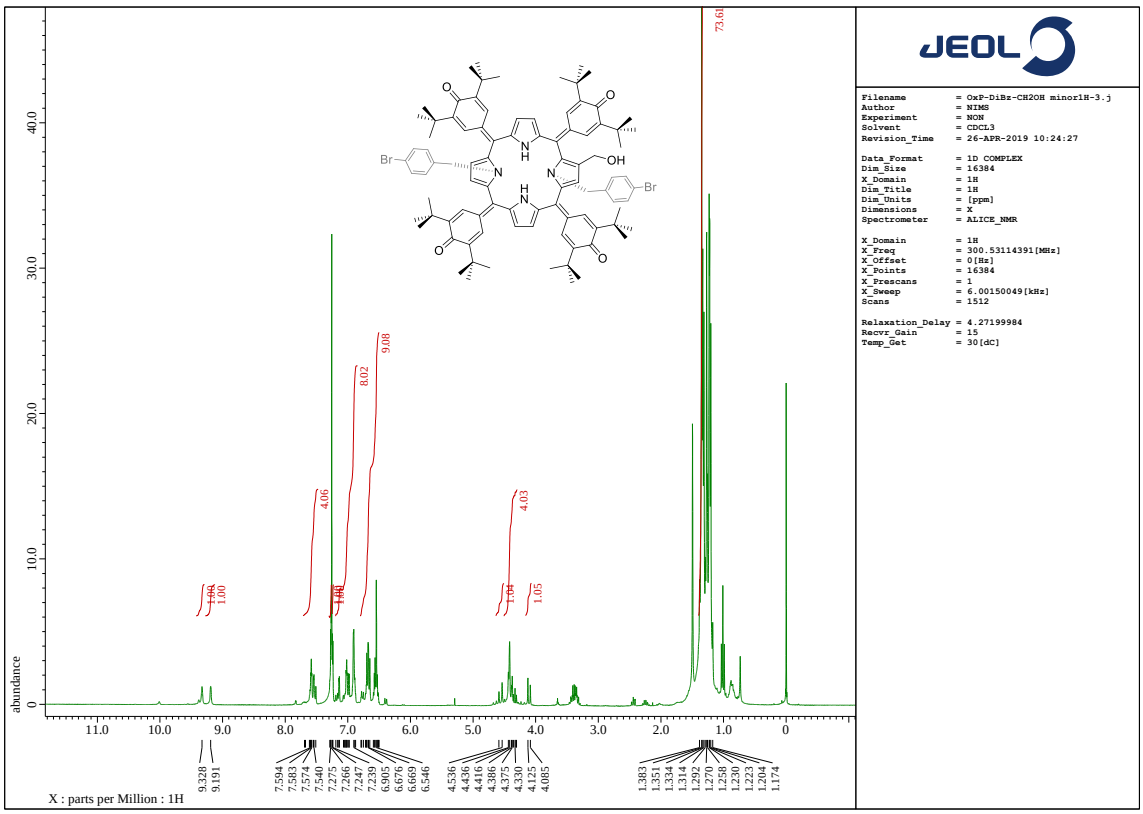

^{1}H NMR spectrum of **Bn_2OxP-CH_2OH Minor** in $CDCl_3$.

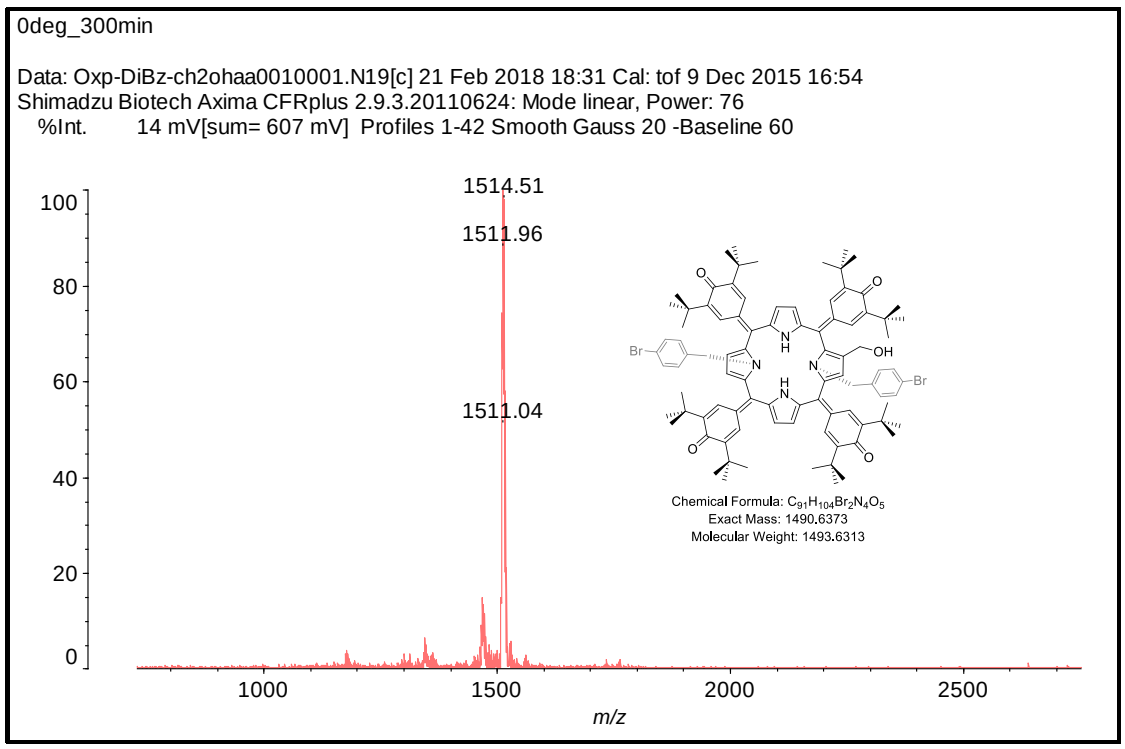

MALDI-TOF-MS mass spectrum of **Bn_2OxP-CH_2OH Minor**.

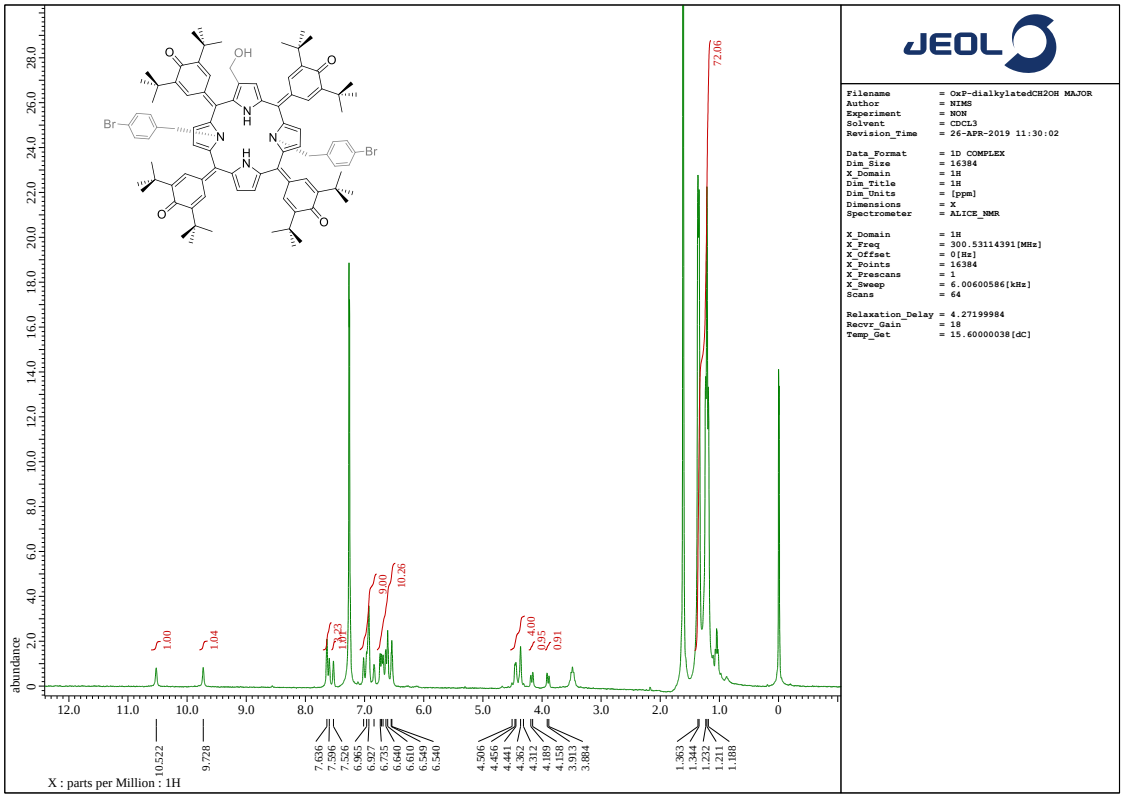

^{1}H NMR spectrum of **Bn$_2$OxP-CH$_2$OH Major** in CDCl$_3$.

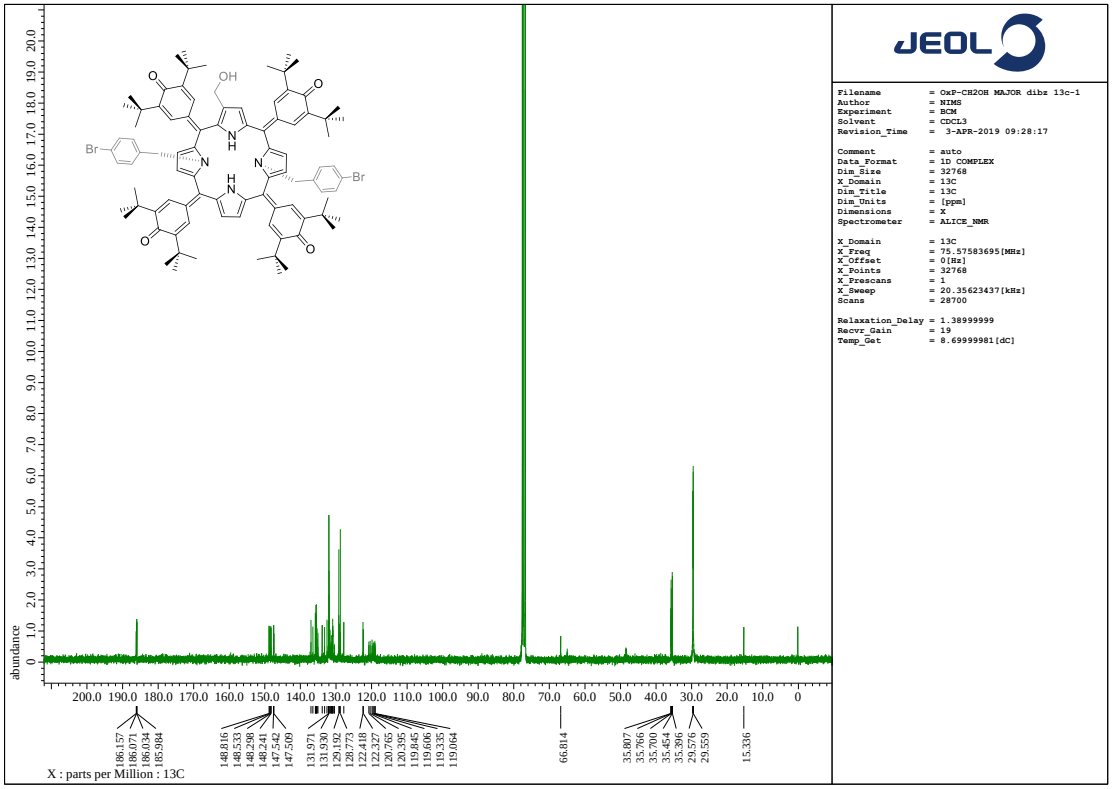

^{13}C NMR spectrum of **Bn$_2$OxP-CH$_2$OH Major** in CDCl$_3$.

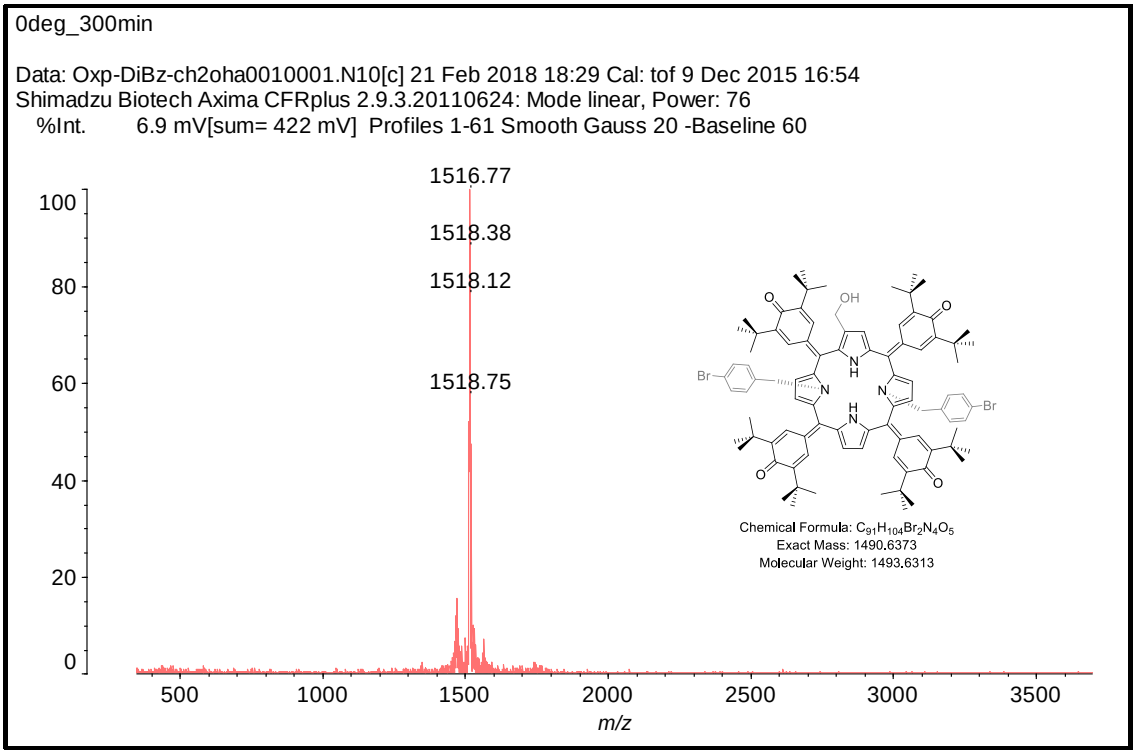

MALDI-TOF-MS mass spectrum of **Bn_2OxP-CH_2OH Major**.

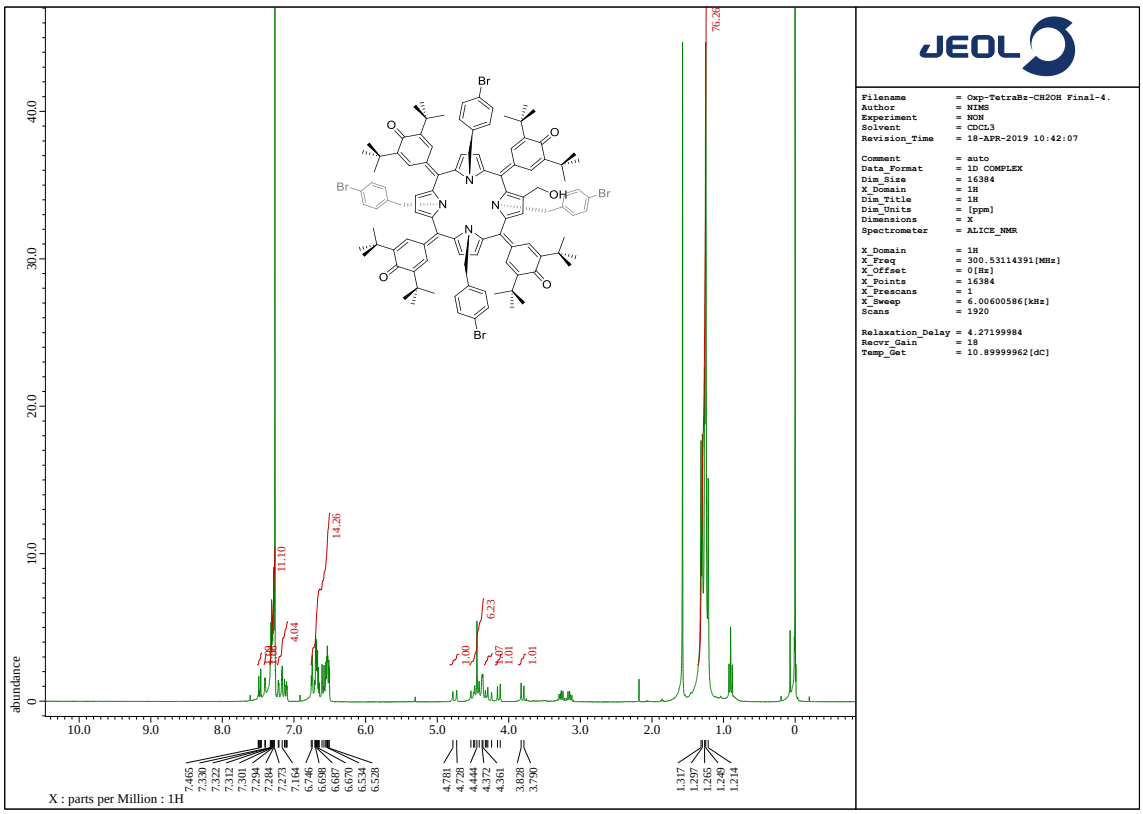

^{1}H NMR spectrum of **Bn$_4$OxP-CH$_2$OH** in CDCl$_3$.

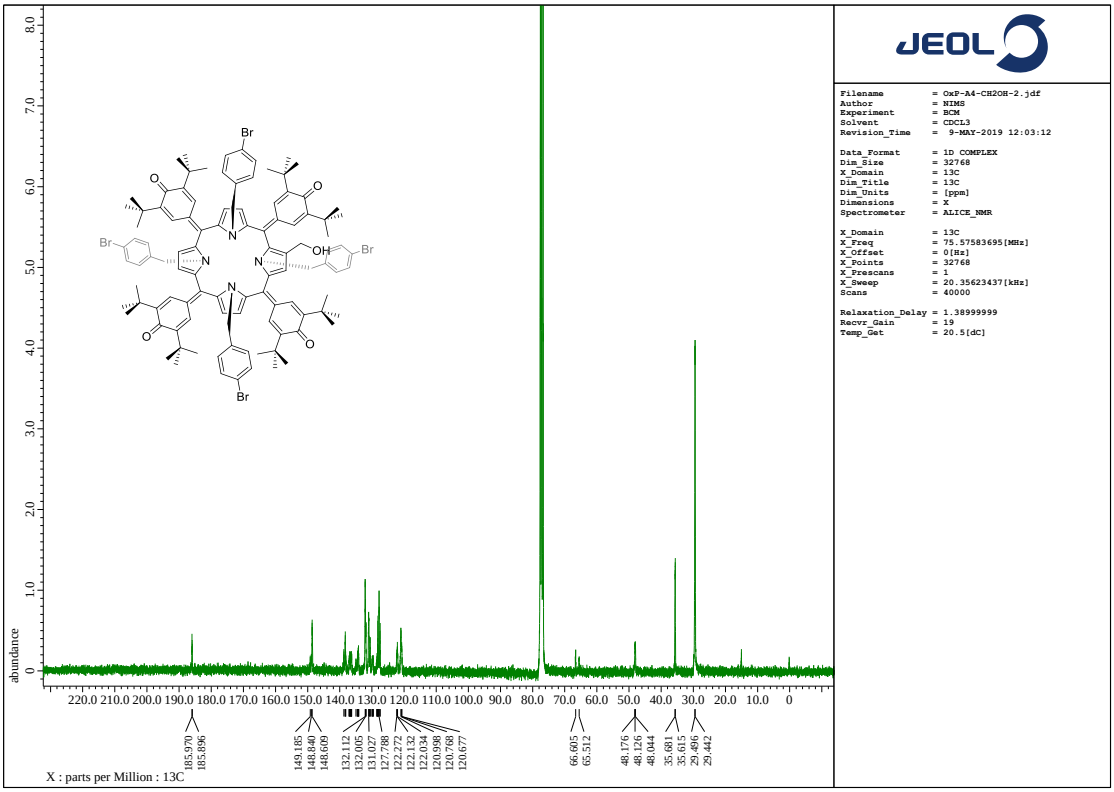

^{13}C NMR spectrum of **Bn$_4$OxP-CH$_2$OH** in CDCl$_3$.

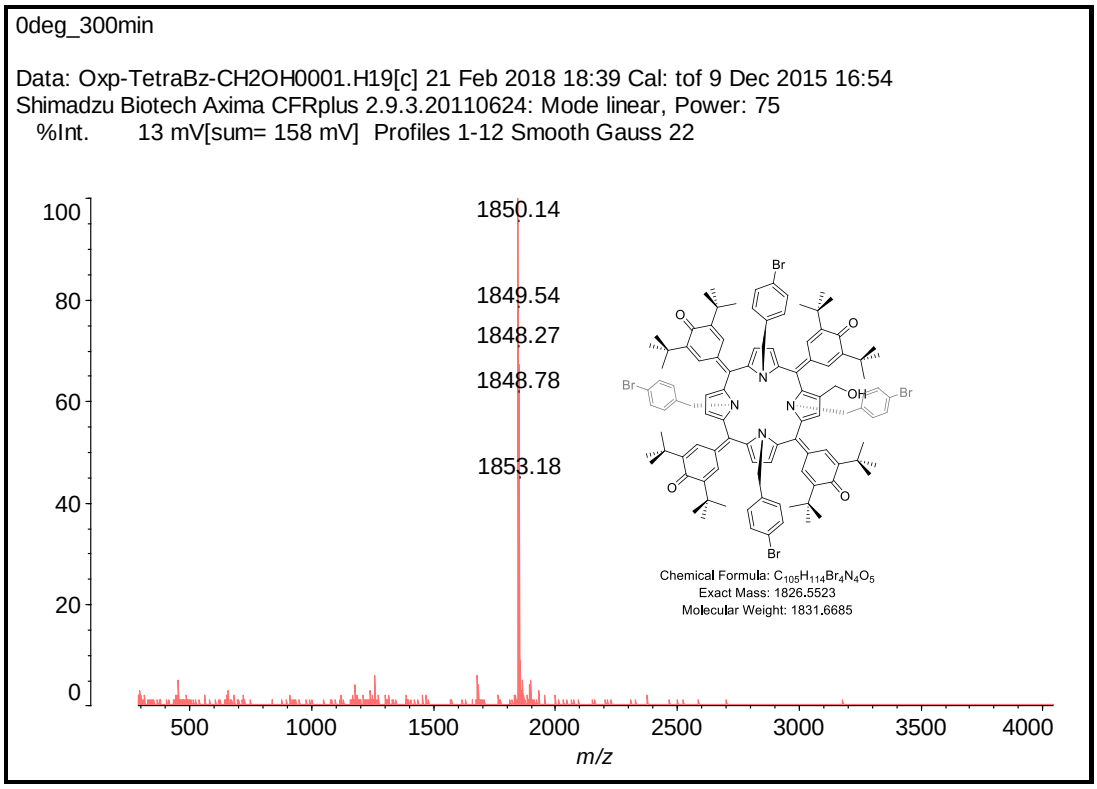

MALDI-TOF-MS mass spectrum of **Bn_4OxP-CH_2OH**.

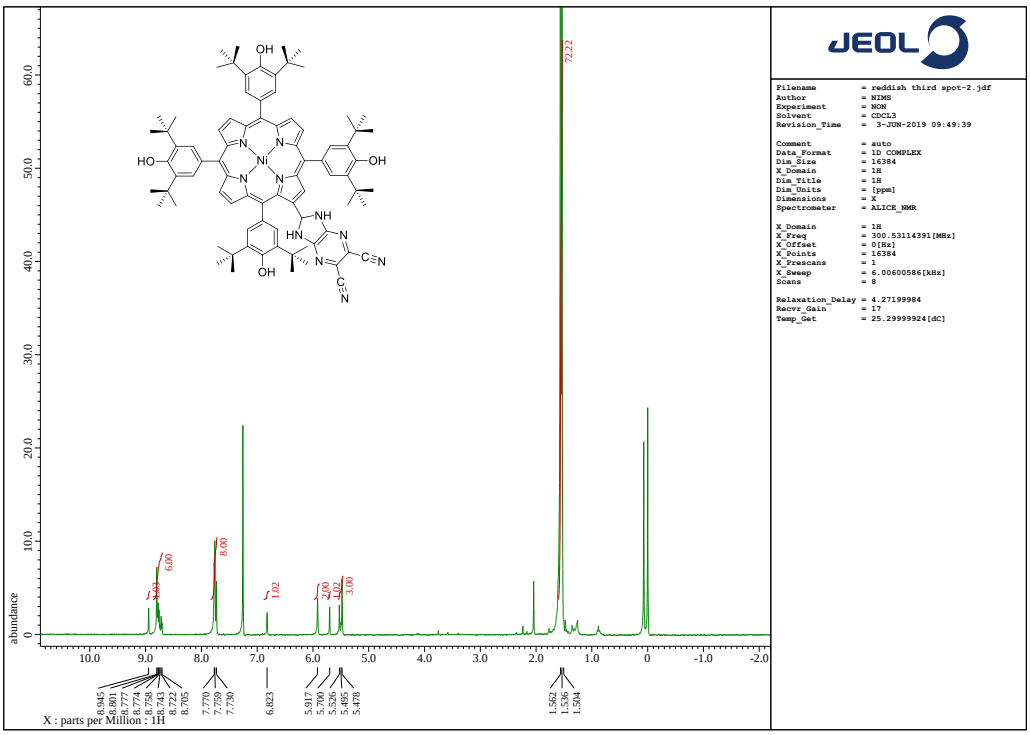

^{1}H NMR spectrum of **3a** in $CDCl_3$.

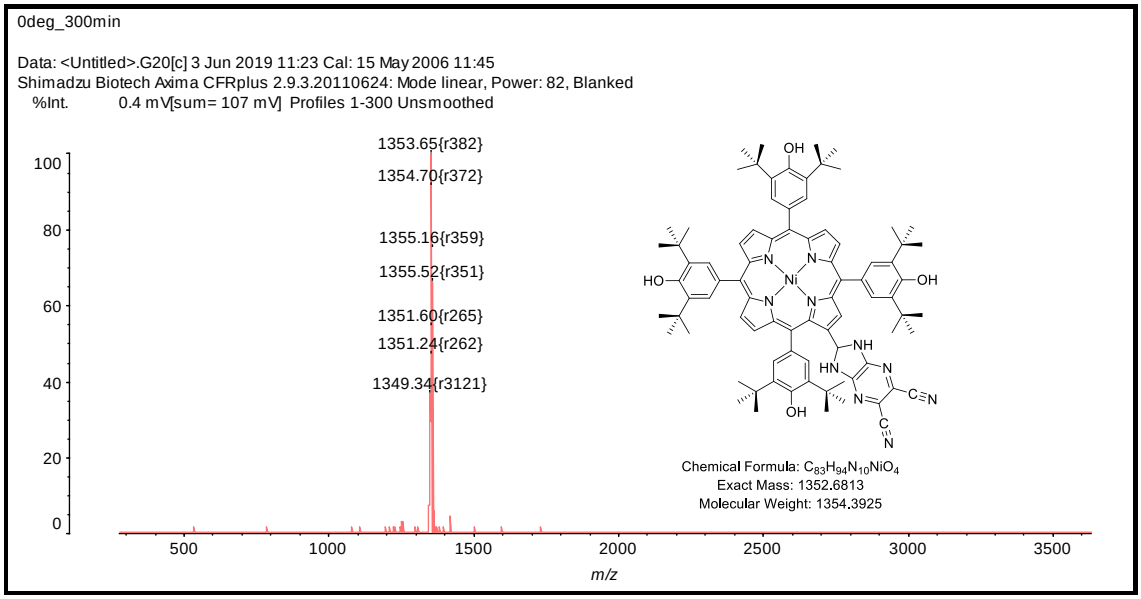

MALDI-TOF-MS mass spectrum of **3a**.

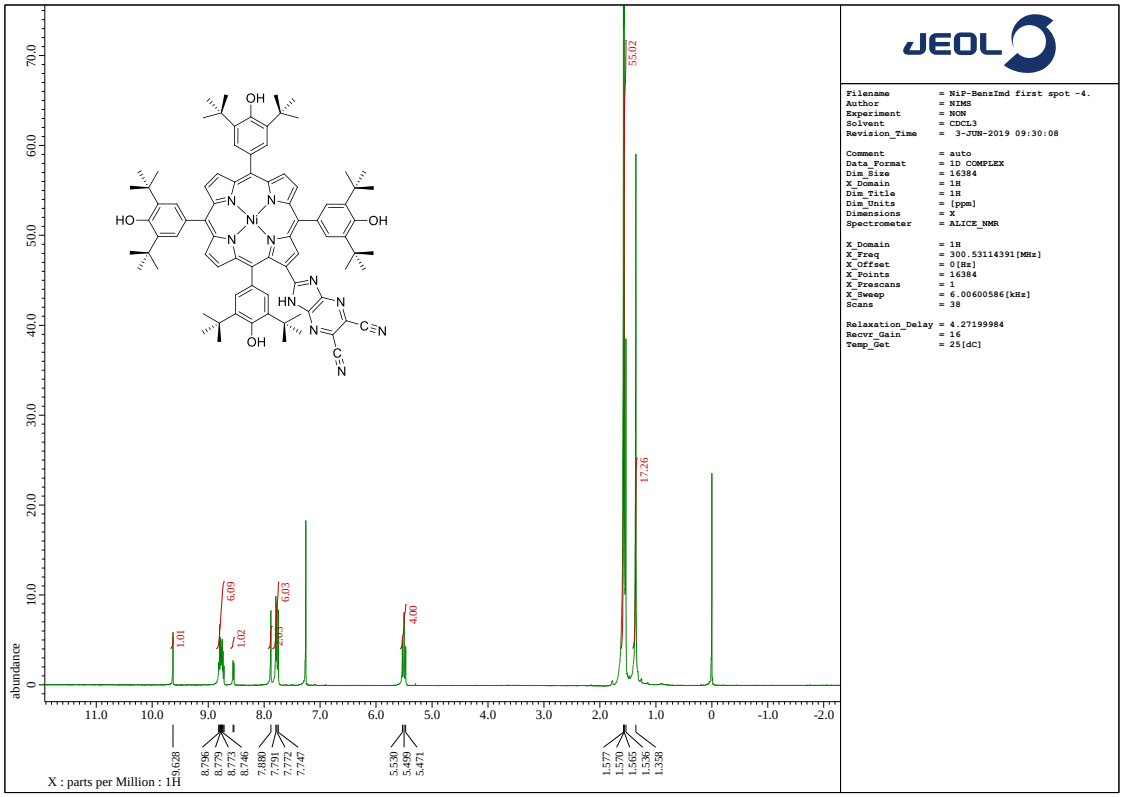

^{1}H NMR spectrum of **3b** in $CDCl_3$.

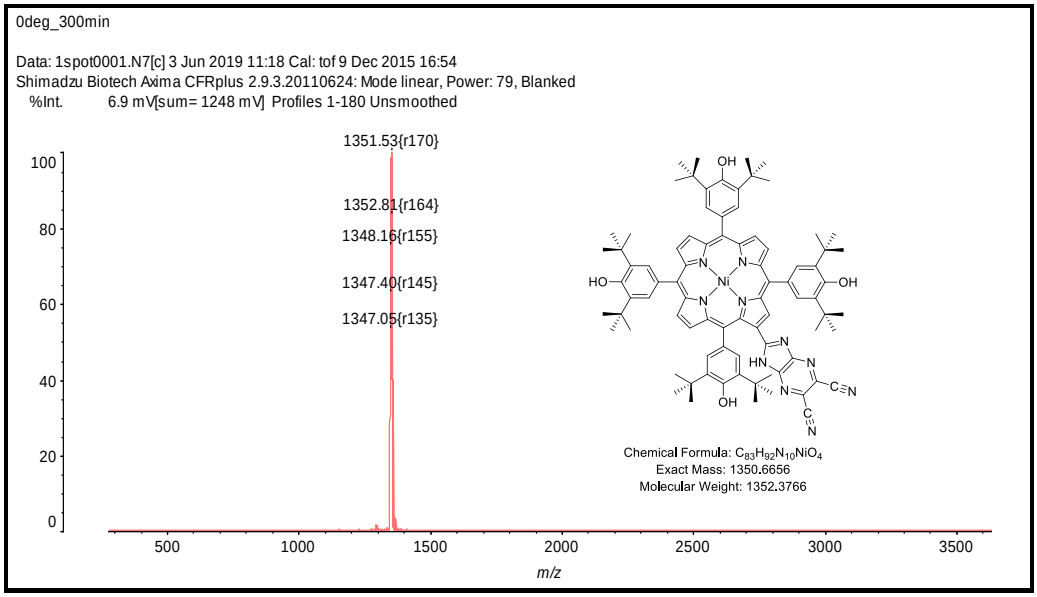

MALDI-TOF-MS mass spectrum of **3b**.

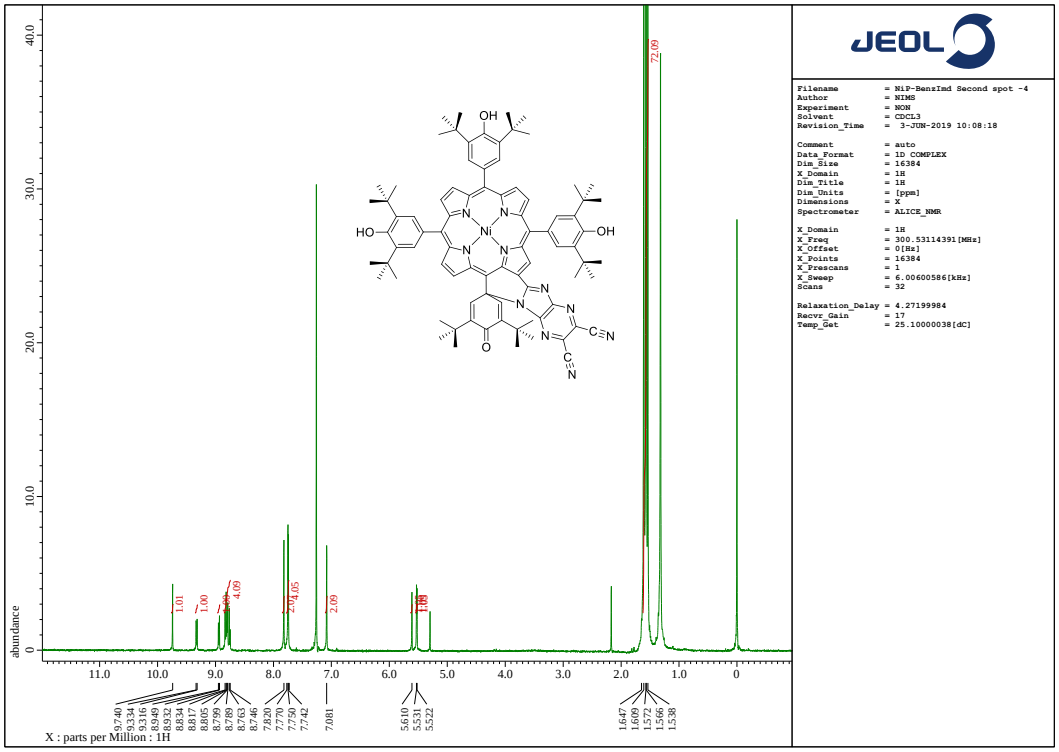

Figure S28.

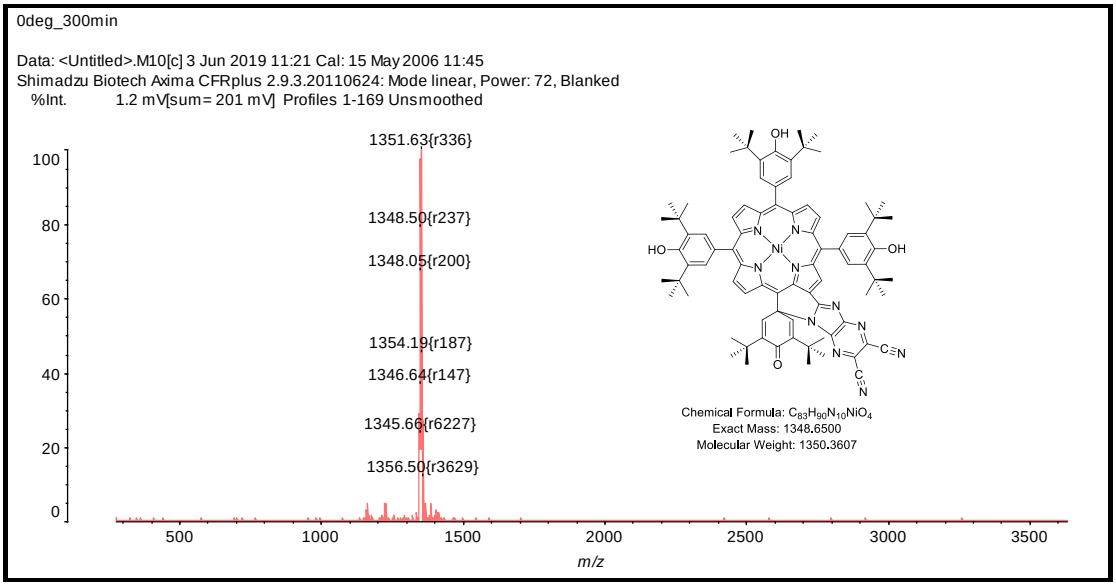

MALDI-TOF-MS mass spectrum of **3c**.